Novel Fluorinated Derivatives of the Broad-Spectrum MMP Inhibitors *N*-Hydroxy-2(*R*)-[[(4-methoxyphenyl)sulfonyl](benzyl)- and (3-picolyl)-amino]-3-methyl-butanamide as Potential Tools for the Molecular Imaging of Activated MMPs with PET

Stefan Wagner,*[,†,‡,#] Hans-Jörg Breyholz,[†,‡,#] Marilyn P. Law,[‡,#] Andreas Faust,[‡,#] Carsten Höltke,[‡,#] Sandra Schröer,[‡,#] Günter Haufe,[§,#] Bodo Levkau,[||,#] Otmar Schober,[‡,#] Michael Schäfers,[‡,⊥,#] and Klaus Kopka[‡,#]

Department of Nuclear Medicine, University Hospital of the Westfälische Wilhelms-Universität Münster, Germany, Institute of Organic Chemistry, University of Münster, Münster, Germany, Institute of Pathophysiology, Center of Internal Medicine, University Hospital, Essen, Germany, Interdisciplinary Center of Clinical Research (IZKF), Münster, Germany, and European Institute of Molecular Imaging (EIMI), Münster, Germany

Received July 13, 2007

An approach to the *in vivo* imaging of locally upregulated and activated matrix metalloproteinases (MMPs) found in many pathological processes is offered by positron emission tomography (PET). Hence, appropriate PET radioligands for MMP imaging are required. Here, we describe the syntheses of novel fluorinated MMP inhibitors (MMPIs) based on lead structures of the broad-spectrum inhibitors *N*-hydroxy-2(*R*)-[[(4-methoxyphenyl)sulfonyl](benzyl)-amino]-3-methyl-butanamide (CGS 25966) and *N*-hydroxy-2(*R*)-[[(4-methoxyphenyl)sulfonyl](3-picolyl)-amino]-3-methyl-butanamide (CGS 27023A). Additionally, tailor-made precursor compounds for radiolabeling with the positron-emitter ^{18}F were synthesized. All prepared hydroxamate target compounds showed high *in vitro* MMP inhibition potencies for MMP-2, MMP-8, MMP-9, and MMP-13. As a consequence, the promising fluorinated hydroxamic acid derivative **1f** was resynthesized in its ^{18}F-labeled version via two different procedures yielding the potential PET radioligand **[^{18}F]1f**. As expected, the biodistribution behavior of this novel compound and that of the more hydrophilic variant **[^{18}F]1j**, also developed by our group, indicates that there was no tissue specific accumulation in wild-type (WT) mice.

Introduction

Matrix metalloproteinases (MMPs[a]) are a family of zinc- and calcium-dependent endopeptidases. The family of MMPs is able to degrade all protein components of the extracellular matrix (ECM) with overlapping substrate specificities and is subdivided into several subclasses.[1−4]

MMPs are secreted as inactive proenzymes or zymogens. Proteolytic cleavage of the prodomain results in the release of the cysteine residue from the zinc ion and in the subsequent activation of the enzyme. This mechanism is termed "cysteine switch".[5] MMP activity is tightly controlled by several endogenous inhibitors, for example, the four tissue inhibitors of metalloproteinases (TIMPs).[6,7]

MMPs and TIMPs are involved in the normal physiology of connective tissue during development, morphogenesis, and wound healing. Elevated MMP expression and activity has been found in numerous disease processes, including inflammation, tumor cell metastasis, and atherosclerosis.[8] Increases in MMP activity in inflammatory, malignant, and degenerative diseases have been attributed to increased cytokine and growth-factor-stimulated gene transcription, enhanced zymogen activation, and an imbalance in the MMP-to-TIMP ratio.[9] The impact of MMPs, especially in tumor progression and metastasis, has led to the development of a number of different synthetic matrix metalloproteinase inhibitors (MMPIs) that block the activated enzyme in pathological conditions by chelating the active site zinc(II) ion of the MMP with a metal complexing moiety (e.g., carboxylic or hydroxamic acid).[10] Synthetic MMPIs available for the treatment of degenerative diseases are hydroxamate based pseudopeptides (e.g., batimastat or marimastat)[11,12] and nonpeptidyl sulfonamide-based hydroxamic acid inhibitors (e.g., AG 3340).[13] Beside this therapeutical application, MMPIs are potentially useful for the noninvasive *in vivo* imaging of activated MMPs with techniques used in diagnostic nuclear medicine (e.g., single photon emission computed tomography (SPECT) and positron emission tomography (PET)). Therefore, radiolabeled analogues of MMPIs can serve as radiotracers for the detection of unbalanced MMP levels. Such improved diagnosis of diseases associated with dysregulated MMP activity would be of great clinical interest and would strongly influence therapy and diagnosis algorithms.

One approach for the imaging of activated MMPs is based on the application of labeled peptides or proteins acting as MMPIs.[14−19]

Another approach is based on the application of radiolabeled small molecule nonpeptidyl MMPIs. Most developments of radiolabeled MMPIs are based on the synthesis and *in vitro* as

* To whom correspondence should be addressed. Address: Department of Nuclear Medicine, University Hospital of the Westfälische Wilhelms-Universität, Albert-Schweitzer-Str. 33, D-48149 Münster, Germany. Phone: +49-251-83-47362. Fax: +49-251-83-47363. E-mail: stwagner@uni-muenster.de.

† These authors contributed equally to this work.

‡ Department of Nuclear Medicine, University Hospital, Münster.

§ Institute of Organic Chemistry, University of Münster.

|| University Hospital, Essen.

⊥ Interdisciplinary Center of Clinical Research (IZKF).

European Institute of Molecular Imaging (EIMI).

[a] Abbreviations: EDC, *N*-ethyl-*N*′-(3-dimethylaminopropyl)-carbodiimide hydrochloride; EM, exact mass; EOS, end of synthesis; ESI, electron spray ionization; HOBt, 1-hydroxy-benzotriazole; K 222, Kryptofix 2.2.2; MMP, matrix metalloproteinase; MMPI, matrix metalloproteinase inhibitor; NMM, 4-methyl-morpholine; PET, positron emission tomography; p.i., post injection; SD, standard deviation; SPECT, single photon emission computed tomography; WT, wild-type.

10.1021/jm0708533 CCC: $37.00
Published on Web 10/23/2007

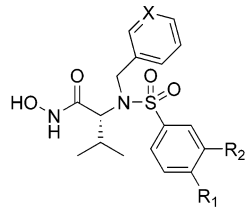

CGS 25966,	X: CH,	R_1: OCH_3,	R_2: H
CGS 27023A,	X: N,	R_1: OCH_3,	R_2: H
[^{123}I]I-HO-CGS 27023A,	X: N,	R_1: OH,	R_2: ^{123}I
[^{11}C]CGS 25966,	X: CH,	R_1: $O^{11}CH_3$,	R_2: H
[^{18}F]1c,	X: N,	R_1: ^{18}F,	R_2: H
[^{18}F]1j,	X: N,	R_1: $OCH_2CH_2{}^{18}F$,	R_2: H

Figure 1. Lead structures of CGS 25966 and CGS 27023A with a selection of radiolabeled derivatives.

well as *in vivo* evaluation of such nonpeptidyl tracers, and they were reviewed recently.[20] In this second group, the *N*-sulfonyl amino acid hydroxamates CGS 25966 and CGS 27023A represent prominent lead structures for potential radiolabeled tracers (Figure 1). The lead compounds CGS 25966 and CGS 27023A are broad-spectrum inhibitors that inhibit MMP-1 (interstitial collagenase, K_i = 43 and 33 nM, respectively), MMP-2 (gelatinase A, K_i = 11 and 20 nM, respectively), MMP-3 (stromelysin-1, K_i = 34 and 43 nM, respectively), and MMP-9 (gelatinase B, K_i = 27 and 8 nM, respectively) by chelating the zinc ion of the enzyme active site with the hydroxamic acid moiety.[21,22]

Lately, our group synthesized a SPECT-compatible ^{123}I-labeled derivate of CGS 27023A ([^{123}I]I-HO-CGS 27023A) for the assessment of MMPs *in vitro* and *in vivo* (Figure 1). This compound was successfully used to image specifically *in vivo* activated MMPs in vascular lesions developing after carotid artery ligation in apolipoprotein E-deficient (ApoE$^{-/-}$) mice by means of planar scintigraphy. This was the first published *in vivo* experiment demonstrating that upregulated MMP levels can be detected with appropriate radiotracers and may provide a new diagnostic parameter in nuclear medicine.[23,24] In the next step, our group and others focused on the development of PET-compatible CGS 25966 and CGS 27023A derivatives labeled with the positron emitters ^{11}C and ^{18}F. To date, several CGS 25966 and CGS 27023A derivatives, mainly labeled with ^{11}C, have been synthesized as potential PET tracers for activated MMPs in breast cancer.[25−28] However, only [^{11}C]CGS 25966 (Figure 1) has been studied in two animal models of breast cancer. Due to unpromising results arising from these studies, [^{11}C]CGS 25966 was excluded from further *in vivo* evaluations.[29] Furthermore, only two ^{18}F-labeled derivatives of CGS 25966 and CGS 27023A have been mentioned in the literature. In 2001, compound **[^{18}F]1c** (Figure 1) was introduced without giving detailed information about the synthesis. To date, *in vitro* and *in vivo* evaluations of **[^{18}F]1c** have not been published.[25,26] Recently, our group succeeded in the synthesis of another ^{18}F-labeled CGS 27023A analogue with a 2-fluoroethoxy subunit **[^{18}F]1j** (Figure 1) via a three-step radiosynthesis. The nonradioactive counterpart **1j** was found to be a potent inhibitor of MMP-2 and MMP-9 (IC_{50} = 3 nM (MMP-2), IC_{50} = 7 nM (MMP-9)).[30]

The work presented here focuses on the systematic investigation of further new fluorinated derivatives of CGS 25966 and CGS 27023A, that should also be achievable as corresponding ^{18}F-labeled isotopomers via fast radiosyntheses starting with the most prominent ^{18}F-labeling species [^{18}F]fluoride ([^{18}F]F$^-$). Therefore, the nonradioactive counterparts and potential precursor compounds of the ^{18}F-labeled analogues were synthesized. These hydroxamic acids **1a**−**f**, **1h**, and **1j**−**n** were tested *in vitro* in MMP-2, -8, -9, and -13 fluorogenic assays and compared with selected carboxylic acid analogues **5a**−**c**, **5f**, and **5h**−**l** occurring in our synthesis sequences, because compounds containing a carboxylic acid moiety that functions as the zinc complexing group and a suitable substitution pattern can show MMPI potency as well.[1]

Additionally, the optimized radiosynthesis of **[^{18}F]1f** is shown. Compound **1f** was identified as one of the most potent MMPIs of our new library (Table 1). Futhermore, the biodistribution of **[^{18}F]1f** was investigated in wild-type (WT) mice side-by-side with that of the more hydrophilic variant **[^{18}F]1j**.

Results

Chemistry. From the (radio)chemical point of view, the introduction of fluorine into the CGS lead structure is only meaningful for distinct molecule positions because the radiochemical synthesis of the corresponding ^{18}F-labeled isotopomers from potential precursor compounds most often is realized with the labeling species [^{18}F]F$^-$ that is frequently used in nucleophilic substitutions. Therefore, the nonradioactive CGS derivatives with a radiochemically meaningful fluorine substitution pattern and the precursor compounds for nucleophilic ^{18}F-fluorination were initially synthesized to investigate their *in vitro* MMP inhibition potencies in enzyme assays and to select suitable candidates for resynthesis of the radioactive ^{18}F-labeled isotopomers. The synthesized fluorinated CGS 25966 and CGS 27023A derivatives and their potential precursor compounds can be classified in three groups.

The *first group* is represented by the corresponding core-fluorinated analogues **1a** and **1c** characterized by a fluorine substitution at the phenyl ring in *para*-position to the electron withdrawing sulfonamide group (Scheme 1). The synthesis of the nonradioactive CGS derivatives **1a** and **1c**, based on the modification of D-valine, is depicted in Scheme 1. The sulfonamide **3a** was derived from the commercially available *tert*-butylester of D-valine hydrochloride **2** and 4-fluorobenzenesulfonyl chloride in the presence of pyridine (yield: 94%). The phenyl or picolyl group was introduced to give the intermediates **4a** and **4c**, respectively (yields: 72−73%), followed by the acidic removal of the ester protective group (yields: 49−79%). Conversion of the resulting carboxylic acids **5a** and **5c** into the corresponding hydroxamic acid esters **6a** and **6d** was achieved by reaction with *O*-*tert*-butylhydroxylamine hydrochloride, *N*-ethyl-*N*′-(3-dimethylaminopropyl)-carbodiimide hydrochloride (EDC), 1-hydroxy-benzotriazole (HOBt), and 4-methyl-morpholine (NMM) (yields: 78−87%). Deprotection of the hydroxamic acid esters **6a** and **6d** was, once again, performed by treatment with hydrochloric acid gas, yielding the target compounds **1a** and **1c** (yields: 31−82%).

Potential precursor compounds of the ^{18}F-labeled analogues **[^{18}F]1a** and **[^{18}F]1c** possess a suitable leaving group for a nucleophilic substitution with [^{18}F]F$^-$ (e.g., $-NO_2$, $-NMe_3{}^+$). Therefore, the syntheses of the corresponding trimethylammonium- and nitro-CGS precursors were achieved. Additionally, the dimethylamino derivatives **1b** and **1d** were synthesized for comparative investigations in the enzyme assays.

Suitable precursors for the substitution of the trimethylammonium group with [^{18}F]F$^-$ should still feature the *O*-*tert*-butyl-protective group, because the acidic deprotection of this moiety with hydrochloric acid would lead to an undesired cleavage of the trimethylammonium group, making a subsequent ^{18}F-fluorination impossible. In detail, the hydroxamic acid esters

Scheme 1. Syntheses of MMPIs **1a**−**1n**[a]

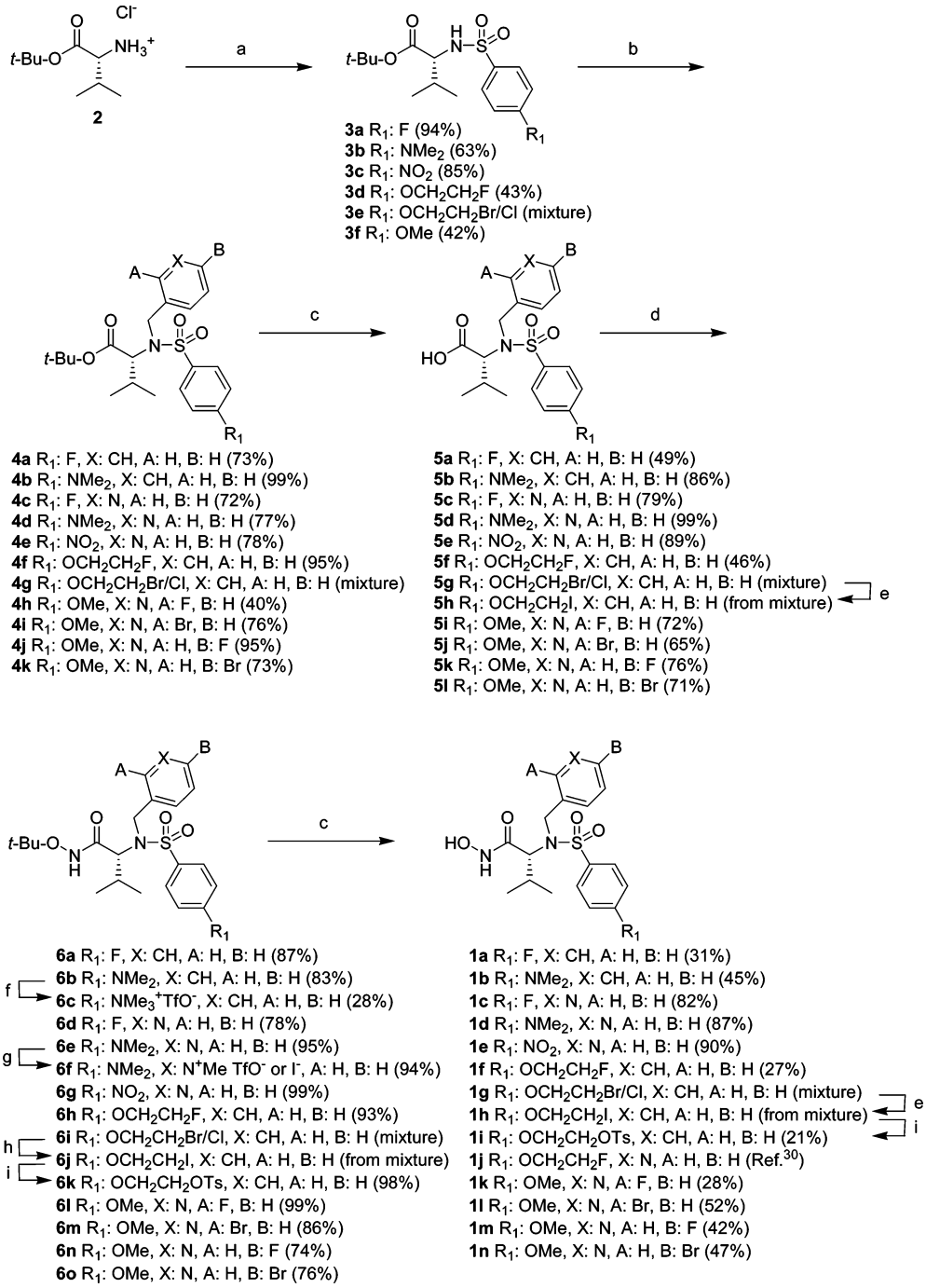

[a] Reagents: (a) 4-R_1-$PhSO_2Cl$, pyridine; (b) benzylbromide, 3-picolyl chloride, 3-bromomethyl-2-fluoropyridine, 2-bromo-3-bromomethylpyridine, 5-bromomethyl-2-fluoropyridine or 2-bromo-5-bromomethylpyridine, K_2CO_3, DMF; (c) HCl, dichloroethane; (d) *t*-Bu-ONH_2, EDC, NMM, HOBt, CH_2Cl_2; (e) NaI, 2-butanone; (f) MeOTf, CH_2Cl_2, CH_3CN; (g) MeOTf, solvent or MeI, CH_2Cl_2; (h) NaI, acetone; (i) AgOTs, CH_3CN.

6b and **6e**, synthesized in analogy to the above-mentioned sequence (Scheme 1, overall yields: 31−46%), were quaternized with methyltriflate or methyliodide. While the quaternization of **6b** yielded the desired trimethylammonium salt **6c** (yield: 28%) (Scheme 1), the *N*-methylation of **6e** under various reaction conditions always led to the undesired methylpyridinium compound **6f** (yield: 94%) (Scheme 1).

However, the synthesis of the nitro-substituted CGS 27023A derivative **1e**, that also represents a potential precursor of **[^{18}F]1c**, was successful via the general synthesis route with a high overall yield of 53%.

The *second group* of fluorinated CGS 27023A and CGS 25966 analogues is characterized by a 2-fluoroethoxy subunit that displaces the methoxy moiety of the lead compounds. The CGS 25966 analogue **1f** was prepared in a five-step procedure with 5% overall chemical yield (Scheme 1). The CGS 27023A analogue **1j** and its ^{18}F-radiolabeled isotopomer **[^{18}F]1j** were prepared by our group as described previously.[30] A potential precursor for a two-step radiosynthesis of **[^{18}F]1f** was synthesized via the chloro/bromo compound mixture **3e**, that was formed in the first synthesis step from the reaction of D-valine-*tert*-butylester hydrochloride **2** and 4-(2-bromoethoxy)-benzenesulfonyl chloride. Obviously, the unintended synthesis of the chloro dervivative in the mixture **3e** arises from the nucleophilic substitution of the bromine in the bromoethoxy core with chloride that descended from compound **2** and/or

Scheme 2. Synthesis of Radiolabeled MMPI **[^{18}F]1f**[a]

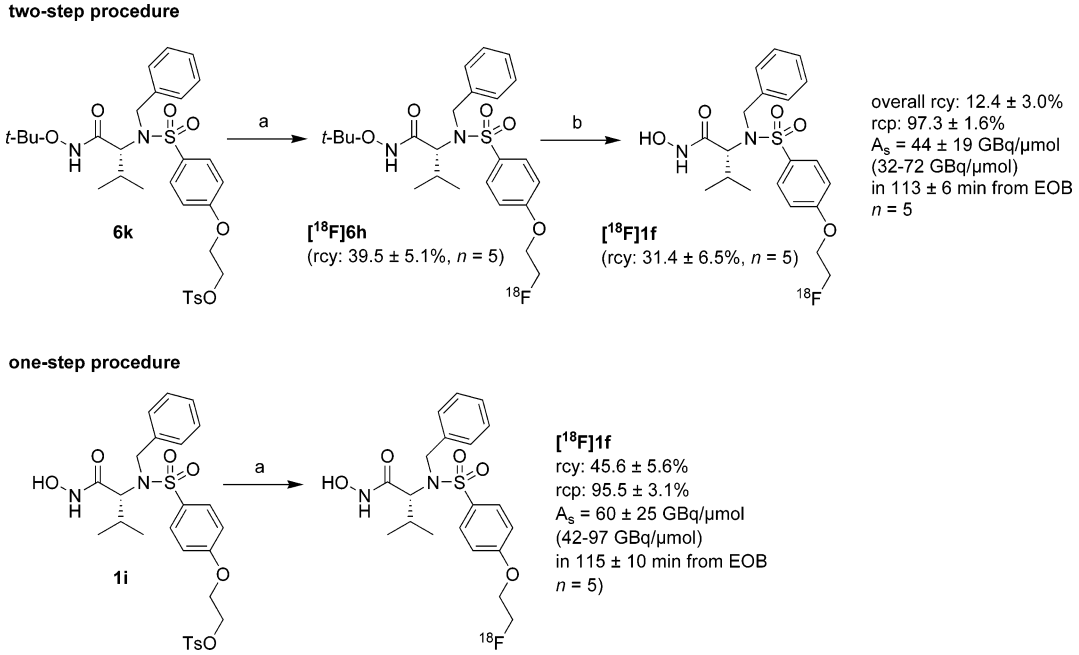

[a] Reagents: (a) [^{18}F]K(K 222)F, K_2CO_3, CH_3CN; (b) TFA.

the benzenesulfonyl chloride derivative. Nevertheless, the mixture **3e** is suitable for the synthesis of the desired corresponding hydroxamic acid ester mixture **6i**. Mixture **6i** was iodinated to provide **6j**, which was subsequently tosylated to yield precursor **6k** (Scheme 1, yield: 98%). Alternatively, a potential precursor for a one-step radiosynthesis of **[^{18}F]1f** was prepared from the chloro/bromo compound mixture **1g**. Subsequent iodination and tosylation yielded the potential tosyl precursor **1i**.

The *third group* of target compounds is exclusively composed of CGS 27023A derivatives and based on the possibility to introduce [^{18}F]F$^-$ in an electron-deficient aromatic subunit with a nucleofuge group (e.g., a bromo-substituted picolyl subunit).[31] Here, the 2- and 6-fluoro-3-picolyl CGS 27023A derivatives **1k** and **1m** (overall yield: 3−9%) and the potential bromo precursors **1l** and **1n** (overall yield: 8−9%) of the ^{18}F-labeled isotopomers were prepared according to Scheme 1. For that purpose, the pyridine derivatives used in step two (3-bromomethyl-2-fluoropyridine, 2-bromo-3-bromomethylpyridine, 5-bromomethyl-2-fluoropyridine, and 2-bromo-5-bromomethylpyridine) were synthesized according to ref 32.

Radiochemistry. Due to the high *in vitro* MMPI potency of compound **1f** (see the section on enzyme assays), the radiosynthesis of its ^{18}F-labeled analogue **[^{18}F]1f** was developed and optimized (Scheme 2). The radiosyntheses of the remaining ligands **[^{18}F]1a**, **[^{18}F]1c**, **[^{18}F]1k**, and **[^{18}F]1m** are in development.

Two different routes for the preparation of **[^{18}F]1f** were evaluated (a two-step and a one-step procedure). In the two-step procedure, the tosylate precursor **6k** was converted into the ^{18}F-substituted ester intermediate **[^{18}F]6h** using [^{18}F]K-(Kryptofix 2.2.2)F ([^{18}F]K(K 222)F) and potassium carbonate in acetonitrile. Compound **[^{18}F]6h** was produced with a radiochemical yield of 39.5 ± 5.1% (noted as mean ± SD, decay-corrected, $n = 5$). The hydrolysis of **[^{18}F]6h** in trifluoroacetic acid (TFA) resulted in the target compound **[^{18}F]1f** with a radiochemical yield of 31.4 ± 6.5% (decay-corrected, $n = 5$). The overall radiochemical yield of **[^{18}F]1f** for both steps was 12.4 ± 3.0% (decay-corrected). The synthesis was achieved with a radiochemical purity of 97.3 ± 1.6% in 113 ± 6 min from end of radionuclide production and a calculated specific radioactivity of 44 ± 19 GBq/μmol (32−72 GBq/μmol) at the end of synthesis (EOS) ($n = 5$).

Additionally, radiosynthesis of the ligand **[^{18}F]1f** was successfully reduced to a one-step procedure using the tosylate precursor **1i**. Direct nucleophilic substitution of hydroxamic acid **1i** with [^{18}F]fluoride provided **[^{18}F]1f** with a radiochemical yield of 45.6 ± 5.6% (decay-corrected), a radiochemical purity of 95.5 ± 3.1% in 115 ± 10 min from end of radionuclide production, and a calculated specific radioactivity of 60 ± 25 GBq/μmol (42−97 GBq/μmol) at the EOS ($n = 5$). Altogether, both procedures provided the chemically pure radioligand **[^{18}F]1f**. Besides the injection peak the UV-trace of the HPLC quality control of the purified **[^{18}F]1f** fraction showed only an additional peak for the carrier, from which the specific radioactivity was calculated.

Enzyme Assays and log *D* Values. The MMP inhibition potencies of the hydroxamic acids CGS 27023A, **1a**−**1f**, **1h**, and **1j**−**1n** and of the carboxylic acids **5a**−**5c**, **5f**, and **5h**−**5l** were measured in fluorogenic *in vitro* inhibition assays for MMP-2, MMP-8, MMP-9, and MMP-13. The resulting IC_{50}-values for the investigated MMPs were calculated from a nonlinear regression fit of the concentration-dependent reaction rates and were compared to those of the parent compound CGS 27023A. The results are shown in Table 1.

The table also contains the K_i-values of CGS 25966 taken from ref 22 and the calculated log *P* and log *D* values (clog *P* and clog *D*) of the synthesized hydroxamic and carboxylic acids to indicate the changes of lipophilicities caused by the structural modifications of the CGS lead compounds. Additionally, the log*D* values of the radioligands **[^{18}F]1f** and **[^{18}F]1j** were determined experimentally (Table 1 footnotes d and e). Comparison of calculated and experimental log *D* values showed that these data differ in 1−2 units (clog *D* of **1f**: 4.03 versus log *D* of **[^{18}F]1f**: 2.02 and clog *D* of **1j**: 2.53 versus log *D* of **[^{18}F]1j**: 1.34).

Our results verify that CGS 27023A is a potent broad-spectrum inhibitor of the tested MMPs with IC_{50}-values in the

Table 1. MMP Inhibition Potencies of the CGS 25966 and CGS 27023A Derivatives for MMP-2, -8, -9, and -13 Expressed in IC_{50}-Values

	IC_{50} [nM][a]					
cpd	MMP-2	MMP-8	MMP-9	MMP-13	clog P[b]	clog D[b]
CGS 25966	11[c]	13[c]	27[c]		3.81	3.80
CGS 27023A	3 ± 1	2 ± 0.4	6 ± 3	34 ± 12	2.32	2.30
1a	239 ± 154	12 ± 9	281 ± 101	384 ± 147	3.60	3.60
5a	4350 ± 950	754 ± 65	821 ± 253	9140 ± 3280	4.99	1.41
1b	335 ± 45	105 ± 34	614 ± 239	10 ± 1	3.72	3.72
5b	(41 ± 36) × 10^3	(14 ± 11) × 10^3	(15 ± 1) × 10^3	(14 ± 4) × 10^3	5.11	1.56
1c	120 ± 76	228 ± 56	414 ± 122	527 ± 90	2.11	2.10
5c	>10 × 10^4	(71 ± 6) × 10^3	>10 × 10^4	>10 × 10^4	3.50	−0.10
1d	992 ± 105	1200 ± 89	1330 ± 1100	1340 ± 506	2.23	2.22
1e	756 ± 215	14 ± 2	5150 ± 1840	10 ± 0.5	2.00	1.98
1f	4 ± 3	2 ± 1	50 ± 27	11 ± 0.3	4.04	4.03[d]
5f	5590 ± 638	2460 ± 464	1300 ± 114	>10 × 10^4	5.42	1.85
1h	22 ± 9	3 ± 1	69 ± 29	10 ± 5	4.92	4.91
5h	207 ± 28	n.d.[f]	1350 ± 554	n.d.	6.31	2.74
1j	3 ± 1	2 ± 1	7 ± 1	0.8 ± 0.03	2.54	2.53[e]
1k	19 ± 9	18 ± 8	51 ± 24	50 ± 23	2.43	2.41
5i	(20 ± 11) × 10^3	(78 ± 11) × 10^3	(10 ± 5) × 10^3	(41 ± 7) × 10^3	3.81	0.21
1l	30 ± 14	75 ± 7	103 ± 6	59 ± 20	3.12	3.11
5j	9110 ± 1170	7480 ± 2050	(35 ± 1) × 10^3	(34 ± 7) × 10^3	4.51	0.90
1m	8 ± 1	0.9 ± 0.3	0.5 ± 0.1	0.9 ± 0.2	2.43	2.41
5k	(35 ± 1) × 10^3	(22 ± 2) × 10^3	9820 ± 2060	(30 ± 5) × 10^3	3.81	0.21
1n	2 ± 1	20 ± 4	23 ± 8	24 ± 4	3.12	3.11
5l	6120 ± 3400	6760 ± 2440	6930 ± 4110	3260 ± 213	4.51	0.91

[a] Values are the mean ± SD of three assays. [b] log P and log D values were calculated with ACD/Chemsketch Labs 6.00 (log D = log P at physiological pH). [c] K_i-values from ref 22, where SDs are not denoted. [d] Experimental determination of log D for compound **[^{18}F]1f**: 2.02 ± 0.03 (noted as mean ± SD, n = 4). [e] Experimental determination of log D for compound **[^{18}F]1j**: 1.34 ± 0.04 (noted as mean ± SD, n = 4). [f] n.d.: not determined.

low nanomolar range (IC_{50} = 2−34 nM). Compared to this lead structure, the core-fluorinated compound **1a** is less potent and the IC_{50}-values range between 12 and 384 nM. Interestingly, this compound shows a moderate selectivity (20−32 fold) for collagenase 2 (MMP-8, IC_{50} = 12 nM). To a minor extent, this tendency also occurred for the corresponding carboxylic acid **5a** (MMP-8, IC_{50} = 754 nM). Here, a low selectivity for MMP-8 and MMP-9 (∼5−13 fold) is observed in comparison to MMP-2 and MMP-13. The carboxylic acid derivative **5a** shows inhibition potentcies that are decreased by a factor of 3−63 compared to the hydroxamic acid analogue **1a**. This result is not surprising, because the intrinsic binding affinity of bidentate hydroxamates for zinc (of enzyme active sites) is much higher than that of monodentate carboxylates.[1] A different result is pointed out by the compound pair of the dimethylamino-substituted hydroxamate **1b** and carboxylate **5b**. Compound **1b** is also a potent inhibitor (IC_{50} = 10−614 nM) but possesses a 11−61-fold selectivity for collagenase 3 (MMP-13). In contrast, carboxylic acid **5b** shows nonselective binding and only low inhibition potencies with IC_{50}-values in the micromolar range (14−41 μM). The core-fluorinated CGS 27023A derivative **1c** exhibits similar binding potencies for MMP-2, -9 and, -13 (IC_{50} = 120−527 nM) compared to the CGS 25966 counterpart **1a** (IC_{50} = 239−384 nM), but the binding selectivity of derivative **1a** for MMP-8 was not found for **1c**. The corresponding carboxylate **5c** is an ineffective inhibitor of the tested MMPs (IC_{50} = 71 to >100 μM). Furthermore, the dimethylamino hydroxamate **1d** (a CGS 27023A derivative) possesses IC_{50}-values of ∼1 μM (992−1340 nM) and is, in contrast to the CGS 25966 analogue **1b**, not specific for MMP-13. The nitro-substituted hydroxamate **1e** was identified as collagenase-selective MMPI (54−515 fold). In comparison to the lead structure CGS 27023A, compound **1e** remains very potent for MMP-8 and -13 (IC_{50} = 10−14 nM) but its MMP inhibition potency for gelatinases A and B (MMP-2 and -9) is remarkably reduced (IC_{50} = 756−5150 nM).

Such selectivity is not shown by the CGS 25966 type hydroxamate **1f** with a 2-fluoroethoxy subunit that displaces the methoxy moiety of the lead compound. In spite of the introduction of a slightly more sterically demanding group, **1f** conserves the broad-spectrum MMPI potency of the lead structures with low nanomolar IC_{50}-values (2−50 nM). Again, the corresponding carboxylate **5f** clearly exhibits a decreased MMP inhibition potency (26 to >9000-fold) compared to the active hydroxamate analogue **1f**. The halogeno analogue **1h** of compound **1f** with the sterically demanding iodine again leads to broad-spectrum inhibition potencies which are not remarkably influenced by the introduction of the bigger iodine atom (IC_{50} = 3−69 nM). The corresponding carboxylic acid **5h** remains a moderate inhibitor for MMP-2 (IC_{50} = 207 nM). The CGS 27023A derivative **1j** is a very potent inhibitor of the investigated MMPs. This compound is even more potent against MMP-13 compared to the lead structure CGS 27023A (43-fold). Compared to the CGS 25966 counterpart **1f**, compound **1j** shows an increased effective inhibition of MMP-9 and MMP-13 (IC_{50} = 50 versus 7 and 11 versus 0.8 nM, respectively).

The compound groups **1k**−**1n** and **5i**−**5l** are composed of the CGS 27023A derivatives and the corresponding carboxylates that possess a halogen substituent (fluorine or bromine) at the picolyl subunit. In comparison to the lead structure CGS 27023A, the fluorine substitution in **1k** causes a slightly decreased but effective inhibition potency with IC_{50}-values in the low nanomolar range (IC_{50} = 18−51 nM). As expected, the corresponding carboxylate moiety in compound **5i** leads to a dramatic loss of inhibition potency (IC_{50} = 10−78 μM). This behavior is also shown by the carboxylic acids **5j**−**5l** that are ≥100-fold less potent than the related hydroxamic acids **1l**−**1n**. A comparison of the bromo-substituted derivative **1l** with the corresponding fluoro compound **1k** indicates that the introduction of a sterically more demanding bromo atom leads to a slight decrease in the inhibitory effectivity for all tested MMPs (IC_{50} = 18−51 versus 30−103 nM). Additionally, the hydroxamate with a 6-fluoro substituent in the picolyl core **1m** possesses superior inhibition potential compared to the above-mentioned analogue with fluorine at the 2-position **1k** (IC_{50} = 0.5−8 versus 18−51 nM). Compound **1m** is the most potent inhibitor of the here presented compound series with even

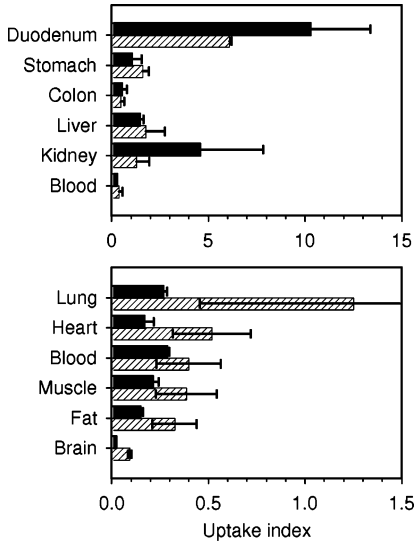

Figure 2. Radioactivity in tissues of mice at 20 min after i.v. injection of **[^{18}F]1f** (solid bar) or **[^{18}F]1j** (slanted stripe bar). Averages for two mice with ranges are shown. The upper panel illustrates uptake in tissues involved with metabolism and excretion (uptake indices 1−15), and the lower panel shows possible target tissues (uptake indices 0.1−1.5). Indices for blood are shown in both panels to assist comparison.

improved IC_{50}-values compared to the lead structure CGS 27023A (IC_{50} = 0.5−8 versus 2−34 nM). The bromo analogue **1n** remains a potent broad-spectrum MMPI with slightly decreased IC_{50}-values for MMP-8, -9, and -13 in comparison to the fluorinated derivative **1m** (IC_{50} = 20 versus 0.9 nM (MMP-8), 23 versus 0.5 nM (MMP-9), and 24 versus 0.9 nM (MMP-13)). In contrast to the fluoro/bromo compound pair **1k** and **1l**, the bromo analogue **1n** is a more effective inhibitor for MMP-2 than the fluoro derivative **1m** (IC_{50} = 2 versus 8 nM (MMP-2)). The comparison of the compound series **1k**−**1n** shows the general tendency that the halogen substitution at the 6-position results in more effective MMP inhibitors than the substitution at the 2-position of the picolyl-ring.

Biodistribution and Metabolism. Figure 2 shows radioactivity in tissue samples of mice at 20 min after intravenous (i.v.) injection of **[^{18}F]1f** or **[^{18}F]1j**. Averages for two mice with ranges are shown. The upper panel illustrates uptake in tissues involved with metabolic and excretory processes (intestinal tract, liver, and kidney), and the lower panel shows possible target tissues (lung, heart, muscle, and brain). The high uptake in the duodenum may be related to the high levels of radioactivity (uptake index: >30) seen in the bile (data not shown). Results for **[^{18}F]1f** and **[^{18}F]1j** were comparable.

Figure 3 illustrates time activity curves for selected tissues. Exponential fits are shown to assist comparison of the data for various tissues. The first sampling time was 2 min after i.v. injection, at which time radioactivity in the blood was low (uptake index: 1.5) and little further change was observed during the next hour. Uptake in the myocardium was comparable to that in the blood for both **[^{18}F]1f** or **[^{18}F]1j**, with there being no evidence for accumulation of radioactivity. Radioactivity was cleared from the tissues which showed high levels at early times after injection. The results for **[^{18}F]1j** in the kidney, however, were very variable; three mice showed uptake indices of ∼7 at 20, 45, and 60 min, while another three mice showed values of ≤1 at the same times, comparable with those for **[^{18}F]1f**. Predosing with unlabeled **1f** or **1j** had no demonstratable effect. Radioactivity was detected in urine at 2 min after injection, and although there was an increase with time, only moderate levels were observed (uptake indices: 8−12 at 60 min). In contrast,

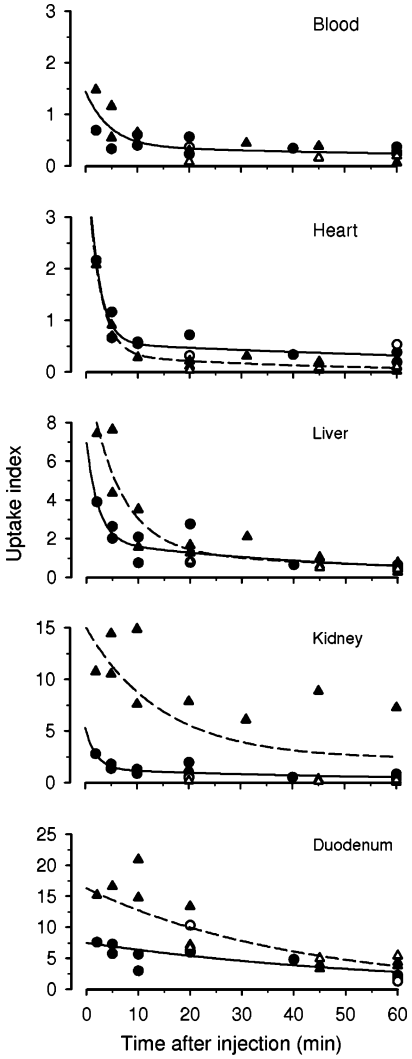

Figure 3. Radioactivity in tissues of mice after i.v. injection of **[^{18}F]1f** or **[^{18}F]1j**. Each symbol indicates an uptake index for one mouse. Compound **[^{18}F]1f** (●) or **[^{18}F]1j** (▲) (13−38 MBq·kg^{-1}, 0.98−4.5 nmol·kg^{-1}) was given alone or 10 min after unlabeled **1f** (○) or **1j** (△), respectively (≥25 μmol·kg^{-1}). As there was no difference between blood activities after injection of **[^{18}F]1f** or **[^{18}F]1j**, a single fit to all data is shown. For other tissues, the solid lines are fitted to all data for **[^{18}F]1f** radioactivity and the broken lines are fitted to all data for **[^{18}F]1j**.

very high levels of radioactivity were detected in the bile for both compounds. Uptake indices ranged from 13 at 2 min after injection to 23−89 between 45 and 60 min.

Additionally, plasma samples of WT mice 2.5 and 20 min postinjection (p.i.) of **[^{18}F]1f** or **[^{18}F]1j** were analyzed by high-performance liquid chromatorgraphy (HPLC). After 2.5 min, 86% of the remaining plasma radioactivity originated from **[^{18}F]1f** and 14% originated from a polar metabolite detected in the γ-trace (trace of radioactivity) of the HPLC chromatogram. After 20 min, the plasma radioactivity was divided into three fractions. In detail, 37% of **[^{18}F]1f** was left, the percentage of the polar metabolite increased to 21%, and in addition a second metabolite with a similar retention time to the parent compound **[^{18}F]1f** occurred (42%). The picolyl derivative **[^{18}F]1j** showed a different behavior. After 2.5 min, the ratio of intact **[^{18}F]1j** to a polar metabolite in plasma was 6/4. The amount of the polar metabolite increased to 47%, and that of **[^{18}F]1j** decreased to 53% of radioactivity remaining in the plasma 20 min p.i. To get an idea about the extent of tracer defluorination and generation of [^{18}F]F$^-$ that accumulates *in vivo* in the skeleton,

the uptake indices of the right tibiae in comparison to those of the heart were determined for the above-mentioned WT mice 20 min after injection of **[^{18}F]1f** or **[^{18}F]1j**. After injection of **[^{18}F]1f**, an uptake index for the tibiae of 0.37 ± 0.10 (n = 4) was observed. In each case, the percentage of injected dose of the tibiae was even lower than that of the heart (0.72 ± 0.11, n = 4). Similar results were provided by the study with **[^{18}F]-1j**. The uptake index was 0.17 ± 0.02% for the heart and 0.12 ± 0.02% for the right tibiae (n = 4).

Discussion

Most of the ^{123}I-, ^{11}C-, and ^{18}F-labeled MMPI radioligands synthesized so far are based on nonpeptidyl MMPIs with carboxylate or hydroxamate moieties as zinc binding functionalities. The radioligand [^{123}I]I-HO-CGS 27023A (Figure 1) which was evaluated by our group represents the first designed radiotracer with moderate lipophilicity (calculated log D = 1.60 (pH 7.4)) that specifically accumulates in vascular MMP-9-rich lesions of apolipoprotein-deficient mice (ApoE$^{-/-}$).[24] The specific accumulation can be observed despite lower potencies (experimental data of ref 23: IC_{50} = 153 nM (MMP-9)) in comparison with the parent compound CGS 27023A (Table 1: IC_{50} = 6 nM (MMP-9)). The aim of our present study was the development of an improved CGS 25966/CGS 27023A-based radioligand that possesses high inhibition potencies for gelatinases and collagenases and, at the same time, can be labeled with the positron emitter ^{18}F using a straightforward radiosynthesis. Subsequently, nonradioactive CGS derivatives with a fluorine substituent were synthesized (Scheme 1). The fluorine substitution pattern of these compounds was chosen in a manner that a radiochemical resynthesis by nucleophilic ^{18}F-fluorination should be possible. Thus, six new fluorinated CGS 25966 and CGS 27023A derivatives (**1a**, **1c**, **1f**, **1j**, **1k**, and **1m**) were prepared in five steps with overall chemical yields ranging between 3 and 34%. Inhibition potencies of compounds were investigated in fluorogenic MMP inhibition assays for MMP-2, -8, -9, and -13. Additionally, nine potential precursors for syntheses of the corresponding ^{18}F-labeled radioligands were prepared, that serve for a one-step (one-step precursor) or two-step radiosynthesis (two-step precursor) (overall chemical yields in 4−7 steps: 8−58%). In detail, trimethylammonium compound **6c** was prepared as a two-step precursor for the radiosynthesis of the potential PET MMPI **[^{18}F]1a**, nitro compounds **6g** and **1e** were obtained as two- or one-step precursors for ^{18}F-fluorinations giving **[^{18}F]1c**, tosylates **6k** and **1i** were synthesized as two- or one-step precursors for the CGS 25966 derivative **[^{18}F]1f**, and bromo compounds **6m**, **1l**, **6o**, and **1n** were prepared as two- or one-step precursors for the synthesis of the CGS 27023A analogues **[^{18}F]1k** and **[^{18}F]1m**, respectively. Syntheses of the precursor, nonradioactive reference **1j** and radioligand **[^{18}F]1j** were already described by our group elsewhere.[23,30] As a result of our *in vitro* evaluation (see below for discussion), we have chosen the potent inhibitor **1f** for synthesis of its ^{18}F-labeled counterpart **[^{18}F]1f**. Two alternative approaches for the radiosynthesis of **[^{18}F]1f** were successfully developed. In a two-step procedure, target compound **[^{18}F]1f** was prepared from the hydroxamic acid ester **6k** with a moderate radiochemical yield of 12.4 ± 3.0% (decay-corrected) (Scheme 2). An improvement was achieved by realization of a one-step procedure starting from the tosylate **1i** which provided **[^{18}F]1f** with a higher radiochemical yield of 45.6 ± 5.6% (decay-corrected), circumventing the subsequent hydrolysis of the ester function of compound **6k**. The one-step procedure offers the improvement of radiation protection by a feasible setup of a fully automated radiosynthesis of compound **[^{18}F]1f** in a commerially available remotely controlled PET tracer synthesizer. Both procedures were achieved in 113−115 min, which complies with ∼1 half-life of ^{18}F (109.7 min). Compared to the two-step procedure, the one-step approach took the same amount of time because the cartridge purification of the one-step procedure is more time-consuming than that of the two-step synthesis. However, being aware of the time-consuming and challenging preparation of the CGS 27013A-derived MMPI **[^{18}F]1j** (three-step synthesis: radiochemical yield, 13.4 ± 5.3% (decay-corrected); synthesis time, 211 ± 30 min after end of radionuclide production (n = 8)[30]), the radiosynthesis of the CGS 25966 analogue **[^{18}F]1f** presented here was further developed, optimized, and finally simplified, resulting in a faster one-step radiosynthesis characterized by higher radiochemical yields.

Furthermore, the experimental log D value determination of the radioligands **[^{18}F]1f** and **[^{18}F]1j** (Table 1 footnotes d and e) in comparison to the log D value calculation of **1f** and **1j** pointed out that experimental measurements and theoretical calculations exhibit a distinct difference of 1−2 units (clog D of **1f**: 4.03 versus log D of **[^{18}F]1f**: 2.02 and clog D of **1j**: 2.53 versus log D of **[^{18}F]1j**: 1.34). The solubility of the radioligands in the buffer was 10−100-fold increased in comparison to the calculated solubility. Maybe the polar character of a hydroxamate moiety is not considered adequately by the calculation software as in the case for the corresponding carboxylic acids. Nevertheless, the expected tendency of a higher lipophilicity of the phenyl compound **1f** compared to the picolyl derivative **1j** was reflected by the calculations.

The prepared hydroxamic acids and selected carboxylic acids were evaluated in MMP inhibition assays using MMP-2, -8, -9, and -13. For the first time, in this study, the aromatic substituents of the lead structures CGS 25966 and CGS 27023A were varied, resulting in new and valuable results.

First, the hydroxamates of the series are more potent MMP inhibitors than the corresponding carboxylates. In most cases, the MMP inhibition potencies of the carboxylates are ≥10-fold decreased. This result was also found for other MMPI classes, and it is caused by the stronger intrinsic binding affinity of hydroxamates for the active site zinc ion in comparison to that of carboxylates.[1]

Second, the CGS 27023A lead structure tolerates a fluoro or bromo substitution at the picolyl ring. While compounds **1k** and **1l** substituted in 2-position are comparable to CGS 27023A (IC_{50} = 18−103 versus 2−34 nM), the 6-substituted derivatives **1m** and **1n** are even more potent MMP inhibitors for some of the investigated MMPs (IC_{50} = 0.5−24 nM). Furthermore, a fluoro substitution is favored over a bromo substitution. Obviously, a linear substitution pattern at the picolyl ring with a little halogen substituent (**1m**) leads to more attractive and/or less repulsive interactions in the S_2' enzyme pocket (the enzyme pocket that is commonly occupied by the picolyl ring; see, e.g., ref 1) than a nonlinear substitution with a sterically more demanding halogen (**1l**).

Third, the replacement of the methoxy moiety of the phenylsulfonamide substructure (this residue commonly occupies the S_1' enzyme pocket; see, e.g., ref 1) leads to selective MMPIs in three cases, including one core-fluorinated derivative. These results are not expected for derivatives of lead structures that are classical examples of nonselective broad-spectrum MMPIs such as CGS 25966 and CGS 27023A. From our results, the collagenase-selective inhibitors **1a** (MMP-8 selective), **1b** (MMP-13 selective), and **1e** (MMP-8 and MMP-13 selective) were identified. This unexpected selectivity might be caused

by electronic and/or sterical reasons. To clarify this observation, a systematic investigation with appropriate substituted derivatives of the lead compounds has to be carried out, but this is out of the focus of our work.

Fourth, the synthesized fluorinated compounds (**1a**, **1c**, **1f**, **1j**, **1k**, and **1m**) remain potent MMPIs on the basis of the CGS 25966 or CGS 27023A lead structure (IC_{50} = 0.5−527 nM). In this context, they can be classified in an order of increasing MMP inhibition potencies: core-fluorinated analogues **1a** and **1c** < 2-fluoroethoxy compounds **1f** and **1j** ≈ 2- and 6-fluoropicolyl CGS 27023A derivatives **1k** and **1m**. As a consequence, the potent MMPI **1f** was chosen for synthesis of its ^{18}F-labeled counterpart. Additionally, our results suggest compound **[^{18}F]1a** as a suitable candidate for the selective imaging of collagenase 2 (MMP-8).

Ex vivo dissection of WT mice indicates that there was no tissue retention of radioactivity after i.v. injection of either **[^{18}F]1f** or **[^{18}F]1j** (Figure 3). Levels of radioactivity in the gastrointestinal tract, liver, and kidney were initially high but decreased with time after injection. Radioactivity levels in the heart, lung, and muscle were comparable with those in the blood, while brain uptake was negligible (Figure 2). Predosing with unlabeled **1f** or **1j** had no demonstratable effect on biodistrubtion and clearance, suggesting there was no specific binding to MMPs in any of the tissues studied. Indeed, low uptake in normal subjects may be an advantage in the study of inflammation, tumor cell metastasis, and atherosclerosis.

The examination of metabolites in the plasma of WT mice showed only one polar metabolite and the corresponding parent compound **[^{18}F]1f** 2.5 min p.i. The polar metabolite, which is presumably not free [^{18}F]F$^-$ (see next paragraph), likely occurs by phase I metabolism via reaction of **[^{18}F]1f** with oxygenases (e.g., resulting in *O*-dealkylation of the parent compound).[33] An additional metabolite of **[^{18}F]1f** appeared 20 min p.i. in plasma that is slightly more hydrophilic compared with **[^{18}F]1f**. This metabolite is probably generated by phase II metabolism and conjugation reaction by transferases (e.g., glucuronidation or glycine conjugation).[33] However, the parent compound **[^{18}F]1f** is still available 20 min p.i., assuring the putative *in vivo* detection of activated MMPs in diseases associated with MMP upregulation. Similar to radioligand **[^{18}F]1f**, a polar metabolite appeared in the plasma of WT mice 2.5 min p.i. of compound **[^{18}F]1j**, which as the parent compound is also detectable. In contrast to **[^{18}F]1f**, a slightly more hydrophilic metabolite of **[^{18}F]1j** did not occur 20 min p.i., but the parent compound **[^{18}F]1j** was still observable, indicating its MMP detection potential 20 min p.i.

The comparison of the uptake index of the right tibiae to that of the heart indicated that the *in vivo* metabolic formation of [^{18}F]F$^-$ from **[^{18}F]1f** or **[^{18}F]1j** was low because the bone accumulation of radioactivity was negligible for both radioligands. Furthermore, the images of initial small animal PET experiments with these radioligands gave no evidence of radioactivity accumulation in the skeleton coming along with *in vivo* formation of [^{18}F]F$^-$ (data not shown).

Significance

The aim of the present study was the development of radioligands for the molecular imaging of activated MMPs *in vivo* by means of PET. Therefore, the hydroxamate-based MMPI lead structures CGS 25966 and CGS 27023A were systematically modified by introduction of fluorine, resulting in six nonradioactive reference compounds of corresponding potential ^{18}F-labeled PET tracers and nine radiolabeling precursors of these radioligands. The compounds were tested in *in vitro* MMP inhibition assays for their MMP-2, -8, -9, and -13 inhibition potencies, resulting in the identification of a collagenase-selective fluorinated inhibitor **1a** (MMP-8 selective). With exception of compound **1a**, it was shown that all synthesized fluorinated hydroxamates are still potent broad-spectrum MMPIs (IC_{50} = 0.5−527 nM). Due to their excellent *in vitro* inhibition potential, especially the 2-fluoroethoxy compounds **1f** and **1j** and the 2- and 6-fluoropicolyl derivatives **1k** and **1m** are suitable candidates for the setup of radiolabeling procedures. As a consequence, we successfully established the ^{18}F-radiosyntheses of **[^{18}F]1f** and **[^{18}F]1j**. As expected, biodistribution and metabolism studies of both PET-compatible radioligands indicate that there was no tissue specific accumulation in WT mice. Low uptake in normal subjects may be an advantage in the study of activated and dysregulated MMPs.

In summary, the here introduced class of hydroxamate-based MMPI radioligands (e.g., **[^{18}F]1f** and **[^{18}F]1j**) could evolve into an innovative tool to noninvasively image activated MMPs *in vivo* in diseases such as inflammation, cancer, or atherosclerosis.

Experimental Section

General Methods. All chemicals, reagents, and solvents for the syntheses were analytical grade and purchased from commercial sources. The melting points (uncorrected) were determined on a Stuart Scientific SMP3 capillary melting point apparatus. ^{1}H NMR and ^{13}C NMR spectra were recorded on Bruker ARX 300 and AMX 400 spectrometers, respectively. Chemical shifts are reported in parts per million (ppm, δ) relative to tetramethylsilane. Mass spectrometry was performed using a Varian MAT 212 (EI = 70 eV) spectrometer and a Bruker MALDI-TOF−MS Reflex IV (matrix: DHB) instrument. Exact mass analyses were conducted on a Bruker MicroTof apparatus. Elemental analyses were realized by using a Vario EL III analyzer. Radiosyntheses were partly carried out using an automated PET tracer synthesizer (TRACERLab Fx_{FDG} Synthesizer; GE Functional Imaging GmbH). The recorded data were processed by the TRACERLab Fx software (GE Functional Imaging GmbH). Separation and purification of the radiosynthesized compounds were performed by gradient radio-HPLC using a Knauer K-500 and a Latek P 402 pump, a Knauer K-2000 UV-detector (λ = 254 nm), a Crismatec NaI(Tl) Scintibloc 51 SP51 γ-detector, and a Nucleosil 100-10 C18 column (250 × 8 mm^2). Sample injection was carried out using a Rheodyne injector block (type 7125 incl. 1000 μL loop). The recorded data were processed by the NINA version 4.9 software (GE Functional Imaging GmbH). The radiochemical purities and the specific activities were acquired with a radio-HPLC system composed of a Syknm S1021 pump, a Knauer K-2501 UV-detector (λ = 254 nm), a Crismatec NaI(Tl) Scintibloc 51 SP51 γ-detector, a Nucleosil 100-3 C18 column (200 × 3 mm^2), a VICI injector block (type C1 incl. 20 μL loop), and the NINA version 4.8, revision 4 software (GE Functional Imaging GmbH). Unless specified, the coupling constant *J* represents H,H-couplings.

General Procedure for the Synthesis of the (*R*)-2-(*N*-Benzyl-/picolyl-arylsulfonamido)-methylbutanoic Acids (5a−5g and 5i−5l). A solution of the corresponding ester **4a**−**4k** in dichloroethane was cooled to 0 to −10 °C. Hydrochloric acid was bubbled through the solution for 2−4 h. The reaction vessel was sealed, and the mixture was warmed to RT and stirred overnight. Removal of the solvent *in vacuo* as well as subsequent treatment with diethyl ether (or diisopropyl ether) provided the colorless solid products (**5b**−**5e**). Silica gel column chromatography using cyclohexane/ethyl acetate mixtures (2:1 (**5g** and **5l**); 3:2 (**5a**, **5f**, **5i,** **5j**, **5k**)) gave the pure products **5a**, **5i,** **5j**, and **5l** as colorless solids, except for **5f** and mixture **5g** and **5k** which were obtained as viscous yellow oils.

(*R*)-2-(*N*-Benzyl-4-fluorophenylsulfonamido)-3-methylbutanoic Acid (5a). Yield: 49%. mp: 135−136 °C. ^{1}H NMR (300 MHz, $CDCl_3$) δ 7.72 (dd, ^3J = 9.1 Hz, $^4J_{H,F}$ = 5.1 Hz, 2H, H_{Aryl}), 7.32−

7.21 (m, 5H, H_{Aryl}), 7.05 (dd, $^3J = {}^3J_{H,F} = 9$ Hz, 2H, H_{Aryl}), 4.56 (AB system, $^2J = 15.6$ Hz, 2H, CH_2), 4.20 (d, $^3J = 10.5$ Hz, 1H, N−CH), 2.07−1.95 (m, 1H, $CH(CH_3)_2$), 0.91 (d, $^3J = 6.6$ Hz, 3H, $CH(CH_3)_2$), 0.82 (d, $^3J = 6.6$ Hz, 3H, $CH(CH_3)_2$). ^{13}C NMR (75.5 MHz, $CDCl_3$) δ 176.10, 165.17 (d, $|^1J_{C,F}| = 264.1$ Hz), 136.52, 130.49, 130.37, 129.17, 128.57, 127.95, 116.11 (d, $|^2J_{C,F}| = 25.5$ Hz), 66.55, 49.34, 28.52, 19.81, 19.75. ^{19}F NMR (282 MHz, $CDCl_3$) δ −105.36. MS (ESI-EM) *m*/*e*: 388.0973 $(M + Na)^+$ calcd for $C_{18}H_{20}FNO_4SNa$ 388.0989. Anal. ($C_{18}H_{20}FNO_4S$) C, H, N.

(*R*)-2-(*N*-Benzyl-4-(dimethylamino)phenylsulfonamido)-3-methylbutanoic Acid Hydrochloride (5b). Yield: 86%. mp: 166−168 °C. ^{1}H NMR (300 MHz, DMSO-d_6) δ 7.54 (d, $^3J = 9.1$ Hz, 2H, H_{Aryl}), 7.38−7.36 (m, 2H, H_{Aryl}), 7.30−7.21 (m, 3H, H_{Aryl}), 6.77 (d, $^3J = 9.1$ Hz, 2H, H_{Aryl}), 4.51 (AB system, $^2J = 16.4$ Hz, 2H, CH_2), 3.91 (d, $^3J = 10.1$ Hz, 1H, N−CH), 2.98 (s, 6H, $N(CH_3)_2$), 1.84−1.72 (m, 1H, $CH(CH_3)_2$), 0.76 (d, $^3J = 6.5$ Hz, 3H, $CH(CH_3)_2$), 0.63 (d, $^3J = 6.5$ Hz, 3H, $CH(CH_3)_2$). ^{13}C NMR (75.5 MHz, DMSO-d_6) δ 171.45, 152.28, 138.37, 128.74, 128.26, 127.93, 126.99, 125.38, 111.28, 65.94, 48.07, 39.90, 28.15, 19.59, 19.33. MS (MALDI-TOF) *m*/*e*: 413 $[M + Na]^+$, 391 $[M + H]^+$. Anal. ($C_{20}H_{26}N_2O_4S$·1.0HCl) C, H, N.

(*R*)-2-(4-Fluorophenylsulfonamido-*N*-(pyridin-3-ylmethyl))-3-methylbutanoic Acid (5c). Yield: 79%. mp: 199−200 °C. ^{1}H NMR (300 MHz, DMSO-d_6) δ 8.88−8.79 (m, 2H, H_{Aryl}), 8.51 (d, $^3J = 8.6$ Hz, 1H, H_{Aryl}), 8.00 (dd, $^3J = 8.2$ Hz, $^3J = 5.6$ Hz, 1H, H_{Aryl}), 7.92 (dd, $^3J = 9.1$ Hz, $^4J_{H,F} = 5.2$ Hz, 2H, H_{Aryl}), 7.42 (dd, $^3J = {}^3J_{H,F} = 9.0$ Hz, 2H, H_{Aryl}), 4.82 (AB system, $^2J = 17.4$ Hz, 2H, CH_2), 3.99 (d, $^3J = 9.9$ Hz, 1H, N−CH), 2.07−1.93 (m, 1H, $CH(CH_3)_2$), 0.86 (d, $^3J = 6.7$ Hz, 3H, $CH(CH_3)_2$), 0.66 (d, $^3J = 6.7$ Hz, 3H, $CH(CH_3)_2$). ^{13}C NMR (75.5 MHz, DMSO-d_6) δ 171.54, 165.11 (d, $|^1J_{C,F}| = 253.3$ Hz), 144.76, 141.84, 141.37, 138.65, 135.21, 131.02, 126.77, 116.82 (d, $|^2J_{C,F}| = 23.0$ Hz), 66.35, 45.88, 28.31, 19.85, 19.48. ^{19}F NMR (282 MHz, DMSO-d_6) δ −100.58. MS (MALDI-TOF) *m*/*e*: 367 $[M + H]^+$. Anal. ($C_{17}H_{19}FN_2O_4S$) C, H, N.

(*R*)-2-(4-(Dimethylamino)phenylsulfonamido-*N*-(pyridin-3-ylmethyl))-3-methylbutanoic Acid Hydrochloride (5d). Yield: 99%. mp: 146−152 °C. ^{1}H NMR (300 MHz, DMSO-d_6) δ 9.30−9.23 (m, 2H, H_{Aryl}), 8.99 (d, $^3J = 8.3$ Hz, 1H, H_{Aryl}), 8.48 (dd, $^3J = 8.2$ Hz, $^3J = 5.7$ Hz, 1H, H_{Aryl}), 7.80 (d, $^3J = 9.2$ Hz, 2H, H_{Aryl}), 6.98 (d, $^2J = 9.2$ Hz, 2H, H_{Aryl}), 5.02 (AB system, $^2J = 17.5$ Hz, 2H, CH_2), 4.20 (d, $^3J = 9.9$ Hz, 1H, N−CH), 3.25 (s, 6H, $N(CH_3)_2$), 2.27−2.15 (m, 1H, $CH(CH_3)_2$), 1.10 (d, $^3J = 6.6$ Hz, 3H, $CH(CH_3)_2$), 0.93 (d, $^3J = 6.6$ Hz, 3H, $CH(CH_3)_2$). ^{13}C NMR (75.5 MHz, DMSO-d_6) δ 171.94, 153.22, 145.44, 140.42, 139.94, 139.65, 129.26, 126.84, 123.52, 111.31, 65.77, 55.03, 45.20, 28.13, 19.81, 19.34. MS (MALDI-TOF) *m*/*e*: 414 $[M - HCl + Na]^+$, 392 $[M - HCl + H]^+$. Anal. ($C_{19}H_{25}N_3O_4S$·2.3HCl) C, H, N.

(*R*)-2-(4-Nitrophenylsulfonamido)-*N*-(pyridin-3-ylmethyl))-3-methylbutanoic Acid Hydrochloride (5e). Yield: 89%. mp: 200−201 °C. ^{1}H NMR (300 MHz, DMSO-d_6) δ 8.83 (s, 2H, H_{Aryl}), 8.48 (d, $^3J = 8.3$ Hz, 1H, H_{Aryl}), 8.38 (d, $^3J = 8.9$ Hz, 2H, H_{Aryl}), 8.11 (d, $^2J = 8.9$ Hz, 2H, H_{Aryl}), 7.98 (dd, $^3J = 8.1$ Hz, $^3J = 5.6$ Hz, 1H, H_{Aryl}), 4.84 (s, 2H, CH_2), 4.05 (d, $^3J = 9.9$ Hz, 1H, N−CH), 2.19−1.97 (m, 1H, $CH(CH_3)_2$), 0.88 (d, $^3J = 6.6$ Hz, 3H, $CH(CH_3)_2$), 0.67 (d, $^3J = 6.6$ Hz, 3H, $CH(CH_3)_2$). ^{13}C NMR (75.5 MHz, DMSO-d_6) δ 171.23, 150.43, 144.90, 144.12, 141.89, 141.52, 138.14, 129.52, 126.88, 124.85, 66.63, 46.19, 28.30, 19.85, 19.49. MS (ESI-EM) *m*/*e*: 392.0938 $(M - H)^-$ calcd for $C_{17}H_{18}N_3O_6S$ 392.0922.

(*R*)-2-(*N*-Benzyl-4-(2-fluoroethoxy)phenylsulfonamido)-3-methylbutanoic Acid (5f). Yield: 52%. ^{1}H NMR (300 MHz, $CDCl_3$) δ 8.91 (s, br, 1H, COOH), 7.69 (d, $^3J = 8.8$ Hz, 2H, H_{Aryl}), 7.36−7.33 (m, 2H, H_{Aryl}), 7.27−7.23 (m, 3H, H_{Aryl}), 6.90 (d, $^3J = 8.8$ Hz, 2H, H_{Aryl}), 4.74 (dt, $^2J_{H,F} = 47.2$ Hz, $^3J = 7.8$ Hz, 2H, O−CH_2CH_2F), 4.55 (AB system, $^2J = 15.9$ Hz, 2H, CH_2), 4.22 (dt, $^3J_{H,F} = 28.2$ Hz, $^3J = 7.8$ Hz, 2H, O−CH_2CH_2F), 4.09 (d, $^3J = 10.3$ Hz, 1H, N−CH), 2.04−1.92 (m, 1H, $CH(CH_3)_2$), 0.89 (d, $^3J = 6.5$ Hz, 3H, $CH(CH_3)_2$), 0.77 (d, $^3J = 6.9$ Hz, 3H, $CH(CH_3)_2$). ^{13}C NMR (75.5 MHz, $CDCl_3$) δ 175.75, 162.05, 137.22, 132.65, 130.16, 129.29, 128.63, 128.01, 114.85, 81.95 ($|^1J_{C,F}| = 170.6$ Hz), 67.80 ($|^2J_{C,F}| = 20.2$ Hz), 66.54, 49.38, 28.72, 20.02. ^{19}F NMR (282 MHz, $CDCl_3$) δ −223.80. MS (ESI-EM) *m*/*e*: 432.1235 (M + Na)$^+$ calcd for $C_{20}H_{24}FNO_5SNa$ 432.1251.

(*R*)-2-(*N*-Benzyl-4-(2-bromoethoxy)phenylsulfonamido)-3-methylbutanoic Acid and (*R*)-2-(*N*-Benzyl-4-(2-chloroethoxy)-phenylsulfonamido)-3-methylbutanoic Acid (5g) (Mixture). ^{1}H NMR (300 MHz, DMSO-d_6) δ 7.69 (d, $^3J = 8.8$ Hz, 2H, H_{Aryl}), 7.38−7.36 (m, 2H, H_{Aryl}), 7.31−7.23 (m, 3H, H_{Aryl}), 7.06 (d, $^3J = 8.8$ Hz, 2H, H_{Aryl}), 4.55 (AB system, $^2J = 16.3$ Hz, 2H, CH_2), 4.43−3.81 (m, 5H, O−CH_2CH_2X and N−CH), 1.87−1.75 (m, 1H, $CH(CH_3)_2$), 0.78 (d, $^3J = 6.9$ Hz, 3H, $CH(CH_3)_2$), 0.64 (d, $^3J = 6.9$ Hz, 3H, $CH(CH_3)_2$). ^{13}C NMR (75.5 MHz, DMSO-d_6) δ 171.64, 161.50, 138.28, 132.02, 129.89, 128.70, 128.37, 127.52, 115.03, 68.69, 66.44, 48.66, 43.23, 41.88, 31.46, 28.41, 19.86, 19.68.

(*R*)-2-(*N*-((2-Fluoropyridin-3-yl)methyl)-4-methoxyphenylsulfonamido)-3-methylbutanoic Acid (5i). Yield: 72%. mp: 129−131 °C. ^{1}H NMR (300 MHz, $CDCl_3$) δ 8.20−8.06 (m, 2H, H_{Aryl}), 7.72 (d, $^3J = 9.1$ Hz, 2H, H_{Aryl}), 7.22−7.17 (m, 1H, H_{Aryl}), 6.91 (d, $^3J = 9.1$ Hz, 2H, H_{Aryl}), 4.65 (AB system, $^2J = 17.2$ Hz, 2H, CH_2), 4.17 (d, $^3J = 10.1$ Hz, 1H, N−CH), 3.83 (s, 3H, OCH_3), 2.05−1.93 (m, 1H, $CH(CH_3)_2$), 0.94 (d, $^3J = 6.5$ Hz, 3H, $CH(CH_3)_2$), 0.82 (d, $^3J = 6.5$ Hz, 3H, $CH(CH_3)_2$). ^{13}C NMR (75.5 MHz, $CDCl_3$) δ 174.72, 163.31, 160.74 (d, $|^1J_{C,F}| = 234.4$ Hz), 146.25, 142.31, 130.75, 129.83, 121.68, 118.97 (d, $|^2J_{C,F}| = 27.1$ Hz), 114.21, 66.06, 55.75, 41.97, 28.55, 19.95, 19.52. ^{19}F NMR (282 MHz, $CDCl_3$) δ −72.96. MS (ESI-EM) *m*/*e*: 419.1045 (M + Na)$^+$ calcd for $C_{18}H_{21}FN_2O_5SNa$ 419.1047. Anal. ($C_{18}H_{21}FN_2O_5S$) C, H, N.

(*R*)-2-(*N*-((2-Bromopyridin-3-yl)methyl)-4-methoxyphenylsulfonamido)-3-methylbutanoic Acid Hydrochloride (5j). Yield: 65%. mp: 169−171 °C. ^{1}H NMR (300 MHz, $CDCl_3$) δ 11.34 (s, 2H), 8.23 (d, $^3J = 4.9$ Hz, 1H, H_{Aryl}), 8.13 (d, $^3J = 7.7$ Hz, 1H, H_{Aryl}), 7.64 (d, $^3J = 9.0$ Hz, 2H, H_{Aryl}), 7.34 (dd, $^3J = 7.7$ Hz, $^3J = 4.9$ Hz, 1H, H_{Aryl}), 6.85 (d, $^3J = 8.9$ Hz, 2H, H_{Aryl}), 4.63 (AB system, $^2J = 18.7$ Hz, 2H, CH_2), 4.01 (d, $^3J = 9.2$ Hz, 1H, N−CH), 3.75 (s, 3H, OCH_3), 1.80−1.73 (m, 1H, $CH(CH_3)_2$), 0.81 (d, $^3J = 6.8$ Hz, 3H, $CH(CH_3)_2$), 0.70 (d, $^3J = 6.8$ Hz, 3H, $CH(CH_3)_2$). ^{13}C NMR (75.5 MHz, $CDCl_3$) δ 171.81, 163.06, 146.40, 140.59, 138.69, 136.62, 129.99, 129.72, 123.16, 114.07, 65.82, 55.50, 47.78, 28.77, 19.97, 19.20. MS (ESI-EM) *m*/*e*: 479.0233 (M + Na)$^+$ calcd for $C_{18}H_{21}BrN_2O_5SNa$ 479.0247. Anal. ($C_{18}H_{21}BrN_2O_5S$·1.4HCl) C, H, N.

(*R*)-2-(*N*-((6-Fluoropyridin-3-yl)methyl)-4-methoxyphenylsulfonamido)-3-methylbutanoic Acid Hydrochloride (5k). Yield: 76%. ^{1}H NMR (300 MHz, $CDCl_3$) δ 8.72 (s, br, COOH), 8.12 (s, 1H, H_{Aryl}), 8.01−7.59 (m, 1H, H_{Aryl}), 7.66 (d, $^3J = 8.8$ Hz, 2H, H_{Aryl}), 6.88−6.84 (m, 1H, H_{Aryl}), 6.87 (d, $^3J = 8.8$ Hz, 2H, H_{Aryl}), 4.60 (AB system, $^2J = 15.9$ Hz, 2H, CH_2), 4.21 (d, $^3J = 10.6$ Hz, 1H, N−CH), 3.82 (s, 3H, OCH_3), 2.00−1.93 (m, 1H, $CH(CH_3)_2$), 0.94 (d, $^3J = 6.9$ Hz, 3H, $CH(CH_3)_2$), 0.82 (d, $^3J = 6.9$ Hz, 3H, $CH(CH_3)_2$). ^{13}C NMR (75.5 MHz, $CDCl_3$) δ 173.74, 163.13, 162.96 (d, $|^1J_{C,F}| = 242.1$ Hz), 147.27, 142.97, 131.56, 131.25, 129.67, 114.14, 109.39 (d, $|^2J_{C,F}| = 36.3$ Hz), 66.18, 55.74, 45.33, 28.65, 19.68, 19.56. ^{19}F NMR (282 MHz, $CDCl_3$) δ −73.53. MS (ESI-EM) *m*/*e*: 419.1040 (M + Na)$^+$ calcd for $C_{18}H_{21}FN_2O_5SNa$ 419.1047. Anal. ($C_{18}H_{21}FN_2O_5S$·0.1HCl) C, H, N.

(*R*)-2-(*N*-((6-Bromopyridin-3-yl)methyl)-4-methoxyphenylsulfonamido)-3-methylbutanoic Acid (5l). Yield: 71%. mp: 73−74 °C. ^{1}H NMR (300 MHz, $CDCl_3$) δ 9.84 (s, 2H), 8.27 (s, 1H, H_{Aryl}), 7.79−7.75 (m, 1H, H_{Aryl}), 7.60 (d, $^3J = 9.0$ Hz, 2H, H_{Aryl}), 7.41 (d, $^3J = 8.1$ Hz, 1H, H_{Aryl}), 6.84 (d, $^3J = 9.3$ Hz, 2H, H_{Aryl}), 4.59 (AB system, $^2J = 16.1$ Hz, 2H, CH_2), 4.27 (d, $^3J = 10.6$ Hz, 1H, N−CH), 3.82 (s, 3H, OCH_3), 2.03−1.92 (m, 1H, $CH(CH_3)_2$), 0.97 (d, $^3J = 6.4$ Hz, 3H, $CH(CH_3)_2$), 0.87 (d, $^3J = 6.4$ Hz, 3H, $CH(CH_3)_2$). ^{13}C NMR (75.5 MHz, $CDCl_3$) δ 173.78, 163.01, 149.81, 140.59, 139.92, 133.06, 131.55, 129.50, 127.93, 114.17, 65.95, 55.67, 45.38, 28.69, 19.67, 19.09. MS (ESI-EM) *m*/*e*: 479.0239 (M + Na)$^+$ calcd for $C_{18}H_{21}BrN_2O_5SNa$ 479.0247. Anal. ($C_{18}H_{21}BrN_2O_5S$) C, H, N.

(*R*)-2-(*N*-Benzyl-4-(2-iodoethoxy)phenylsulfonamido)-3-methylbutanoic Acid (5h). An amount of 1.60 g (10.6 mmol) of anhydrous

sodium iodide (dried at 100 °C *in vacuo* for 3 h) and 600 mg of compound mixture **5g** in 40 mL of 2-butanone were heated to reflux for 6 days. After cooling to ambient temperature, the solvent was evaporated and the residue was subjected to silica gel column chromatography (cyclohexane/ethyl acetate 3:2), affording 370 mg (0.72 mmol) of pure compound **5h** as a yellow oil, which solidified on standing. mp: 57−59 °C. ^{1}H NMR (400 MHz, $CDCl_3$) δ 7.68 (d, ^3J = 8.7 Hz, 2H, H_{Aryl}), 7.36−7.32 (m, 2H, H_{Aryl}), 7.27−7.23 (m, 3H, H_{Aryl}), 6.86 (d, ^3J = 8.7 Hz, 2H, H_{Aryl}), 4.55 (AB system, ^2J = 15.8 Hz, 2H, CH_2), 4.25 (t, ^3J = 6.9 Hz, 2H, O−CH_2CH$_2$I), 4.16 (d, ^3J = 10.7 Hz, 1H, N−C*H*), 3.39 (t, ^3J = 6.9 Hz, 2H, O−CH$_2$CH_2I), 2.04−1.93 (m, 1H, C*H*(CH$_3$)$_2$), 0.89 (d, ^3J = 6.5 Hz, 3H, CH(CH_3)$_2$), 0.78 (d, ^3J = 6.9 Hz, 3H, CH(CH_3)$_2$). ^{13}C NMR (75.5 MHz, $CDCl_3$) δ 174.96, 161.25, 136.86, 132.54, 129.92, 129.02, 128.31, 127.73, 114.59, 68.86, 66.24, 49.08, 28.44, 19.77, 19.72, 0.21. MS (ESI-EM) *m*/*e*: 516.0362 (M − H)$^+$ calcd for $C_{20}H_{23}INO_5S$ 516.0347.

General Procedure for the Synthesis of the (*R*)-2-(*N*-Benzyl-/picolyl-4-arylsulfonamido)-*N*-hydroxy-3-methylbutanamides (1a−1g and 1k−1n). A solution of the corresponding (*R*)-2-(*N*-benzyl-/picolyl-4-arylsulfonamido)-*N*-*tert*-butyloxy-3-methylbutanamides **6a**, **6b**, **6d**, **6e**, **6g**−**6i**, and **6l**−**6o** in dichloroethane was cooled to −10 °C. Hydrochloric acid was bubbled through the solution for 2−4 h. The reaction vessel was sealed, and the mixture was warmed to ambient temperature and stirred overnight. Removal of the solvent to 1/3 of its original volume *in vacuo* and subsequent treatment with diisopropyl ether provided the colorless solid products. Compounds **1a**, **1f**, and **1k**−**1n** were purified by silica gel column chromatography eluting with cyclohexane/ethyl acetate mixtures (3:2) (**1a** and **1f**), (1:1) (**1m**), (1:2) (**1k**, **1l**, and **1n**), yielding the colorless solid products.

(*R*)-2-(*N*-Benzyl-4-fluorophenylsulfonamido)-*N*-hydroxy-3-methylbutanamide (1a). A solid-phase synthesis of the (*S*)-enantiomer is described in ref 34. Yield: 31%. mp: 166−167 °C. ^{1}H NMR (300 MHz, $CDCl_3$) δ 10.60 (s, 1H, O*H*), 8.36 (s, 1H, N*H*), 7.60 (dd, ^3J = 8.1 Hz, $^4J_{H,F}$ = 5.1 Hz, 2H, H_{Aryl}), 7.34−7.17 (m, 5H, H_{Aryl}), 6.97 (dd, ^3J = $^3J_{H,F}$ = 9 Hz, 2H, H_{Aryl}), 4.71 (s, 2H, CH_2), 3.97 (d, ^3J = 10.8 Hz, 1H, N−C*H*), 2.21−2.09 (m, 1H, C*H*(CH$_3$)$_2$), 0.85 (d, ^3J = 6.5 Hz, 3H, CH(CH_3)$_2$), 0.77 (d, ^3J = 6.5 Hz, 3H, CH(CH_3)$_2$). ^{13}C NMR (75.5 MHz, $CDCl_3$) δ 166.50, 164.65 (d, $|^1J_{C,F}|$ = 254.0 Hz), 136.84, 136.63, 129.89, 129.37, 128.03, 127.38, 115.82 (d, $|^2J_{C,F}|$ = 22.7 Hz), 64.01, 48.60, 28.05, 19.61, 19.61. ^{19}F NMR (282 MHz, $CDCl_3$) δ −106.20. MS (ESI-EM) *m*/*e*: 403.1094 (M + Na)$^+$ calcd for $C_{18}H_{21}FN_2O_4SNa$ 403.1098. Anal. ($C_{18}H_{21}FN_2O_4S$) C, H, N.

(*R*)-2-(*N*-Benzyl-4-(dimethylamino)phenylsulfonamido)-*N*-hydroxy-3-methylbutanamide Hydrochloride (1b). Yield: 45%. mp 98−101 °C (decomposition). ^{1}H NMR (300 MHz, DMSO-d_6) δ 10.77 (s, 1H, O*H*), 8.13 (s, 1H, N*H*), 7.50 (d, ^3J = 8.2 Hz, 2H, H_{Aryl}), 7.37−7.20 (m, 5H, H_{Aryl}), 6.67 (d, ^3J = 8.2 Hz, 2H, H_{Aryl}), 4.60 (AB system, ^2J = 15.7 Hz, 2H, CH_2), 3.79 (d, ^3J = 10.7 Hz, 1H, N−C*H*), 2.96 (s, 6H, N(CH_3)$_2$), 1.85−1.70 (m, 1H, C*H*(CH$_3$)$_2$), 0.71 (d, ^3J = 6.0 Hz, 3H, CH(CH_3)$_2$), 0.62 (d, ^3J = 6.0 Hz, 3H, CH(CH_3)$_2$). ^{13}C NMR (75.5 MHz, DMSO-d_6) δ 175.50, 166.26, 152.58, 138.89, 129.05, 129.95, 128.15, 127.27, 111.44, 63.37, 47.68, 28.53, 19.87, 19.48. (^{13}C NMR signal for N(CH$_3$)$_2$ is not detectable.) MS (ESI-EM) *m*/*e*: 428.1614 (M + Na)$^+$ calcd for $C_{20}H_{27}N_3O_4SNa$ 428.1616. Anal. ($C_{20}H_{27}N_3O_4S$·1.1HCl) C, H, N.

(*R*)-2-(4-Fluorophenylsulfonamido-*N*-(pyridin-3-ylmethyl))-*N*-hydroxy-3-methylbutanamide Hydrochloride (1c). Yield: 82%. mp: 144−145 °C. ^{1}H NMR (300 MHz, DMSO-d_6) δ 10.95 (s, 1H, O*H*), 8.77−8.76 (m, 2H, H_{Aryl}), 8.40 (d, ^3J = 8.2 Hz, 1H, H_{Aryl}), 7.92 (dd, ^3J = 8.1 Hz, ^3J = 5.8 Hz, 1H, H_{Aryl}), 7.88 (dd, ^3J = 8.1 Hz, ^3J = 5.8 Hz, 2H, H_{Aryl}), 7.34 (dd, ^3J = $^3J_{H,F}$ = 9 Hz, 2H, H_{Aryl}), 4.85 (AB system, ^2J = 16.4 Hz, 2H, CH_2), 3.82 (d, ^3J = 10.8 Hz, 1H, N−C*H*), 2.05−1.92 (m, 1H, C*H*(CH$_3$)$_2$), 0.80 (d, ^3J = 6.5 Hz, 3H, CH(CH_3)$_2$), 0.62 (d, ^3J = 6.5 Hz, 3H, CH(CH_3)$_2$). ^{13}C NMR (75.5 MHz, DMSO-d_6) δ 174.93, 164.89 (d, $|^1J_{C,F}|$ = 254.6 Hz), 145.00, 142.08, 141.25, 138.53, 136.11, 130.56, 130.43, 116.78 (d, $|^2J_{C,F}|$ = 23.0 Hz), 64.68, 46.05, 27.59, 19.90, 19.59. ^{19}F NMR (282 MHz, DMSO-d_6) δ −101.05. MS (MALDI-TOF) *m*/*e*: 404 [M + Na]$^+$, 382 [M + H]$^+$. Anal. ($C_{17}H_{20}FN_3O_4S$·1.3HCl) C, H, N.

(*R*)-2-(4-(Dimethylamino)phenylsulfonamido-*N*-(pyridin-3-ylmethyl))-*N*-hydroxy-3-methylbutanamide (1d). Yield: 87%. mp: 147−151 °C. ^{1}H NMR (300 MHz, DMSO-d_6) δ 8.77 (d, ^3J = 5.7 Hz, 1H, H_{Aryl}), 8.74 (s, 1H, H_{Aryl}), 8.46 (d, ^3J = 8.2 Hz, 1H, H_{Aryl}), 7.98 (dd, ^3J = 7.9 Hz, ^3J = 5.7 Hz, 1H, H_{Aryl}), 7.51 (d, ^3J = 8.9 Hz, 2H, H_{Aryl}), 6.69 (d, ^3J = 8.9 Hz, 2H, H_{Aryl}), 4.78 (AB system, ^2J = 17.3 Hz, 2H, CH_2), 3.83 (d, ^3J = 10.7 Hz, 1H, N−C*H*), 2.98 (s, 6H, N(CH_3)$_2$), 2.02−1.90 (m, 1H, C*H*(CH$_3$)$_2$), 0.77 (d, ^3J = 6.3 Hz, 3H, CH(CH_3)$_2$), 0.59 (d, ^3J = 6.3 Hz, 3H, CH(CH_3)$_2$). ^{13}C NMR (75.5 MHz, DMSO-d_6) δ 166.43, 152.76, 145.76, 140.49, 139.70, 139.67, 128.98, 126.82, 124.96, 111.38, 63.42, 52.44, 44.68, 28.51, 19.45, 19.25. MS (ESI-EM) *m*/*e*: 429.1553 (M + Na)$^+$ calcd for $C_{19}H_{26}N_4O_4SNa$ 429.1567.

(*R*)-2-(4-Nitrophenylsulfonamido-*N*-(pyridin-3-ylmethyl))-*N*-hydroxy-3-methylbutanamide (1e). Yield: 90%. mp: 125−126 °C. ^{1}H NMR (300 MHz, DMSO-d_6) δ 11.37 (s, 1H, O*H*), 8.73−8.68 (m, 2H, H_{Aryl}), 8.31 (d, ^3J = 9.0 Hz, 1H, H_{Aryl}), 8.24 (d, ^3J = 8.3 Hz, 2H, H_{Aryl}), 8.02 (d, ^3J = 9.0 Hz, 1H, H_{Aryl}), 7.77 (dd, ^3J = 8.0 Hz, ^3J = 5.5 Hz, 2H, H_{Aryl}), 4.93 (AB system, ^2J = 16.3 Hz, 2H, CH_2), 3.97 (d, ^3J = 10.6 Hz, 1H, N−C*H*), 2.10−1.99 (m, 1H, C*H*(CH$_3$)$_2$), 0.83 (d, ^3J = 6.5 Hz, 3H, CH(CH_3)$_2$), 0.72 (d, ^3J = 6.5 Hz, 3H, CH(CH_3)$_2$). ^{13}C NMR (75.5 MHz, DMSO-d_6) δ 174.26, 165.27, 149.69, 144.80, 143.60, 136.40, 128.54, 125.60, 124.35, 115.46, 63.29, 48.50, 27.78, 19.19, 19.75. MS (EI): *m*/*e* (intensity %): 408 (M$^+$, 6), 348 (4), 250 (6), 235 (16), 207 (11), 125 (100), 82 (59), 55 (30). Anal. ($C_{17}H_{20}N_4O_6S$) C, H, N.

(*R*)-2-(*N*-Benzyl-4-(2-fluoroethoxy)phenylsulfonamido)-*N*-hydroxy-3-methylbutanamide (1f). Yield: 27%. mp: 144−146 °C. ^{1}H NMR (400 MHz, $CDCl_3$) δ 7.60 (m, 2H, H_{Aryl}), 7.37−7.35 (m, 2H, H_{Aryl}), 7.27−7.24 (m, 3H, H_{Aryl}), 6.89 (m, 2H, H_{Aryl}), 4.76 (d, $^2J_{H,F}$ = 49.1 Hz, 2H, O−CH$_2$CH_2F), 4.60 (AB system, ^2J = 15.6 Hz, 2H, CH_2), 4.23 (d, $^3J_{H,F}$ = 27.3 Hz, 2H, O−CH_2CH$_2$F), 3.79 (m, 1H, N−C*H*), 2.23−2.14 (m, 1H, CH−C*H*(CH$_3$)$_2$), 0.81 (d, ^3J = 6.5 Hz, 3H, CH(CH_3)$_2$), 0.55 (d, ^3J = 6.9 Hz, 3H, CH(CH_3)$_2$). ^{13}C NMR (100 MHz, $CDCl_3$) δ 167.15, 161.69, 136.56, 132.33, 129.35, 129.03, 128.10, 127.48, 114.63, 82.20 ($|^1J_{C,F}|$ = 172.7 Hz), 67.33 ($|^2J_{C,F}|$ = 20.4 Hz), 63.72, 48.57, 27.20, 19.57, 19.08. ^{19}F NMR (282 MHz, $CDCl_3$) δ −224.01. MS (ESI-EM) *m*/*e*: 447.1363 (M + Na)$^+$ calcd for $C_{20}H_{25}FN_2O_5SNa$ 447.1360. Anal. ($C_{20}H_{25}FN_2O_5S$) C, H, N.

(*R*)-2-(*N*-Benzyl-4-(2-bromoethoxy)phenylsulfonamido)-*N*-hydroxy-3-methylbutanamide and (*R*)-2-(*N*-Benzyl-4-(2-chloroethoxy)phenylsulfonamido)-*N*-hydroxy-3-methylbutanamide (1g) (Mixture). ^{1}H NMR (300 MHz, DMSO-d_6) δ 10.79 (s, 1H, O*H*), 8.93 (s, 1H, N*H*), 7.61 (d, ^3J = 8.8 Hz, 2H, H_{Aryl}), 7.35−7.32 (m, 2H, H_{Aryl}), 7.25−7.19 (m, 3H, H_{Aryl}), 6.97 (d, ^3J = 8.8 Hz, 2H, H_{Aryl}), 4.66 (AB system, ^2J = 15.7 Hz, 2H, CH_2), 4.40−3.80 (m, 5H, O−CH_2CH_2X and N−C*H*), 1.93−1.80 (m, 1H, C*H*(CH$_3$)$_2$), 0.73 (d, ^3J = 6.5 Hz, 3H, CH(CH_3)$_2$), 0.67 (d, ^3J = 6.5 Hz, 3H, CH(CH_3)$_2$). ^{13}C NMR (75.5 MHz, DMSO-d_6) δ 165.75, 160.81, 137.94, 132.49, 129.17, 128.76, 127.87, 127.05, 114.65, 68.14, 63.17, 47.59, 42.94, 28.11, 19.50, 19.09.

(*R*)-2-(*N*-((2-Fluoropyridin-3-yl)methyl)-4-methoxyphenylsulfonamido)-*N*-hydroxy-3-methylbutanamide (1k). Yield: 28%. mp: 167−169 °C. ^{1}H NMR (300 MHz, DMSO-d_6) δ 10.83 (s, 1H, O*H*), 8.95 (s, 1H, N*H*), 8.07 (s, 1H, H_{Aryl}), 7.90−7.84 (m, 1H, H_{Aryl}), 7.68 (d, ^3J = 9.2 Hz, 2H, H_{Aryl}), 7.25−7.20 (m, 1H, H_{Aryl}), 7.00 (d, ^3J = 9.2 Hz, 2H, H_{Aryl}), 4.72 (AB system, ^2J = 17.1 Hz, 2H, CH_2), 3.80 (d, ^3J = 12.1 Hz, 1H, N−C*H*), 3.82 (s, 3H, OCH_3), 1.98−1.84 (m, 1H, C*H*(CH$_3$)$_2$), 0.77 (d, ^3J = 6.5 Hz, 3H, CH(CH_3)$_2$), 0.67 (d, ^3J = 6.5 Hz, 3H, CH(CH_3)$_2$). ^{13}C NMR (75.5 MHz, DMSO-d_6) δ 165.53, 162.47, 160.17 (d, $|^1J_{C,F}|$ = 237.0 Hz), 145.94, 141.34, 130.98, 129.19, 121.69, 120.28 (d, $|^2J_{C,F}|$ = 29.3 Hz), 114.17, 62.65, 55.63, 40.47, 27.80, 19.32, 18.90. ^{19}F NMR (282 MHz, $CDCl_3$) δ −73.30. MS (MALDI-TOF) *m*/*e*: 434 [M + Na]$^+$, 412 [M + H]$^+$. Anal. ($C_{18}H_{22}FN_3O_5S$) C, H, N.

(*R*)-2-(*N*-((2-Bromopyridin-3-yl)methyl)-4-methoxyphenylsulfonamido)-*N*-hydroxy-3-methylbutanamide (1l). Yield: 52%. mp: 174 °C. ^{1}H NMR (300 MHz, DMSO-d_6) δ 10.81 (s, 1H, O*H*),

8.90 (s, 1H, N*H*), 8.16 (d, ^3J = 4.5 Hz, 1H, H_{Aryl}), 7.68 (d, ^3J = 8.9 Hz, 2H, H_{Aryl}), 7.71−7.64 (m, 1H, H_{Aryl}), 7.28 (dd, ^3J = 7.7 Hz, ^3J = 4.5 Hz, 1H, H_{Aryl}), 7.00 (d, ^3J = 8.9 Hz, 2H, H_{Aryl}), 4.71 (AB system, ^2J = 17.7 Hz, 2H, CH_2), 3.78 (s, 3H, OCH_3), 3.78−3.75 (m, 1H, N−C*H*), 1.87−1.75 (m, 1H, C*H*$(CH_3)_2$), 0.71 (d, ^3J = 6.4 Hz, 3H, CH(CH_3)$_2$), 0.62 (d, ^3J = 6.6 Hz, 3H, CH(CH_3)$_2$). ^{13}C NMR (75.5 MHz, DMSO-d_6) δ 165.38, 162.69, 148.37, 140.89, 138.06, 134.80, 130.61, 129.49, 122.93, 114.32, 62.57, 55.59, 46.80, 27.88, 19.46, 18.92. MS (ESI-EM) *m*/*e*: 496.0332 $(M + Na)^+$ calcd for $C_{18}H_{22}BrN_3O_5SNa$ 496.0337.

(*R*)-2-(*N*-((6-Fluoropyridin-3-yl)methyl)-4-methoxyphenylsulfonamido)-*N*-hydroxy-3-methylbutanamide (1m). Yield: 42%. mp: 156 °C. ^{1}H NMR (300 MHz, DMSO-d_6) δ 10.94 (s, 1H, O*H*), 9.03 (s, 1H, N*H*), 8.09 (s, 1H, H_{Aryl}), 7.85−7.79 (m, 1H, H_{Aryl}), 7.55 (d, ^3J = 8.8 Hz, 2H, H_{Aryl}), 7.01−6.95 (m, 1H, H_{Aryl}), 6.91 (d, ^3J = 8.8 Hz, 2H, H_{Aryl}), 4.67 (AB system, ^2J = 15.8 Hz, 2H, CH_2), 3.86 (d, ^3J = 10.6 Hz, 1H, N−C*H*), 3.80 (s, 3H, OCH_3), 2.01−1.89 (m, 1H, C*H*$(CH_3)_2$), 0.88 (d, ^3J = 6.6 Hz, 3H, CH(CH_3)$_2$), 0.71 (d, ^3J = 6.6 Hz, 3H, CH(CH_3)$_2$). ^{13}C NMR (75.5 MHz, DMSO-d_6) δ 165.88, 162.23, 162.13 (d, $|^1J_{C,F}|$ = 235.6 Hz), 146.25, 147.58, 142.39, 131.93, 128.88, 114.02, 108.63 (d, $|^2J_{C,F}|$ = 38.0 Hz), 62.96, 55.62, 44.18, 27.87, 19.21, 18.93. ^{19}F NMR (282 MHz, $CDCl_3$) δ −71.15. MS (ESI-EM) *m*/*e*: 434.1154 $(M + Na)^+$ calcd for $C_{18}H_{22}FN_3O_5SNa$ 434.1156. Anal. ($C_{18}H_{22}FN_3O_5S$) C, H, N.

(*R*)-2-(*N*-((6-Bromopyridin-3-yl)methyl)-4-methoxyphenylsulfonamido)-*N*-hydroxy-3-methylbutanamide (1n). Yield: 47%. mp: 168−172 °C. ^{1}H NMR (300 MHz, DMSO-d_6) δ 10.92 (s, 1H, O*H*), 9.03 (s, 1H, N*H*), 8.22 (s, 1H, H_{Aryl}), 7.60−7.54 (m, 1H, H_{Aryl}), 7.55 (d, ^3J = 9.0 Hz, 2H, H_{Aryl}), 7.43 (d, ^3J = 8.2 Hz, 1H, H_{Aryl}), 7.68 (d, ^3J = 9.0 Hz, 2H, H_{Aryl}), 4.63 (AB system, ^2J = 16.0 Hz, 2H, CH_2), 3.85 (d, ^3J = 10.8 Hz, 1H, N−C*H*), 3.81 (s, 3H, OCH_3), 2.00−1.88 (m, 1H, C*H*$(CH_3)_2$), 0.78 (d, ^3J = 6.5 Hz, 3H, CH(CH_3)$_2$), 0.70 (d, ^3J = 6.5 Hz, 3H, CH(CH_3)$_2$). ^{13}C NMR (75.5 MHz, DMSO-d_6) δ 165.86, 162.29, 150.42, 139.80, 139.63, 133.38, 131.79, 128.92, 127.16, 114.05, 62.93, 55.63, 44.36, 27.86, 19.23, 18.92. MS (ESI-EM) *m*/*e*: 494.0361 $(M + Na)^+$ calcd for $C_{18}H_{22}BrN_3O_5SNa$ 494.0356. Anal. ($C_{18}H_{22}BrN_3O_5S$) C, H, N.

(*R*)-2-(*N*-Benzyl-4-(2-iodoethoxy)phenylsulfonamido)-*N*-hydroxy-3-methylbutanamide (1h). An amout of 794 mg (5.58 mmol) of anhydrous sodium iodide (dried at 100 °C *in vacuo* for 3 h) and 1.20 g of compound mixture **1g** in 30 mL of 2-butanone were heated to reflux overnight. After cooling to room temperature, the solvent was evaporated and the residue was subjected to silica gel column chromatography (cyclohexane/ethyl acetate 2:1), affording 550 mg (1.03 mmol) of compound **1h** as a colorless foam. mp: 140−142 °C. ^{1}H NMR (300 MHz, $CDCl_3$) δ 9.19 (s, 1H, O*H*), 7.58 (d, ^3J = 9.0 Hz, 2H, H_{Aryl}), 7.36−7.32 (m, 2H, H_{Aryl}), 7.27−7.23 (m, 3H, H_{Aryl}), 6.87 (d, ^3J = 9.0 Hz, 2H, H_{Aryl}), 4.57 (AB system, ^2J = 16.1 Hz, 2H, CH_2), 4.27 (t, ^3J = 6.9 Hz, 2H, O−CH_2CH$_2$I), 3.74 (d, ^3J = 10.7 Hz, 1H, N−C*H*), 3.42 (t, ^3J = 6.9 Hz, 2H, O−CH$_2$CH_2I), 2.25−2.12 (m, 1H, C*H*$(CH_3)_2$), 0.80 (d, ^3J = 6.4 Hz, 3H, CH(CH_3)$_2$), 0.52 (d, ^3J = 6.4 Hz, 3H, CH(CH_3)$_2$). ^{13}C NMR (75.5 MHz, $CDCl_3$) δ 167.32, 161.25, 136.55, 132.43, 129.53, 129.18, 128.30, 127.70, 114.83, 68.81, 63.72, 48.67, 27.19, 19.80, 19.21, 0.08. MS (ESI-EM) *m*/*e*: 555.0404 $(M + Na)^+$ calcd for $C_{20}H_{25}IN_2O_5SNa$ 555.0421.

(*R*)-2-(*N*-Benzyl-4-(2-(tosyloxy)ethoxy)phenylsulfonamido)-*N*-hydroxy-3-methylbutanamide (1i). An amount of 2.80 g (10.0 mmol) of silver tosylate and 550 mg of compound **1h** in 60 mL of acetonitrile were heated to reflux overnight. After cooling to ambient temperature, the solvent was evaporated and the residue was subjected to silica gel column chromatography (cyclohexane/ethyl acetate 1:1), affording 120 mg (0.208 mmol) of compound **1i** as a colorless foam. Yield: 21%. mp: 101−104 °C. ^{1}H NMR (300 MHz, $CDCl_3$) δ 9.13 (s, 1H, N*H*), 7.84 (d, ^3J = 8.3 Hz, 2H, H_{Aryl}), 7.55 (d, ^3J = 8.9 Hz, 2H, H_{Aryl}), 7.37−7.25 (m, 7H, H_{Aryl}), 6.78 (d, ^3J = 8.9 Hz, 2H, H_{Aryl}), 4.57 (AB system, ^2J = 15.3 Hz, 2H, CH_2), 4.39−4.36 (m, 2H, O−CH$_2$CH$_2$OTs), 4.20−4.17 (m, 2H, O−CH$_2$CH$_2$OTs), 3.70 (d, ^3J = 10.8 Hz, 1H, N−C*H*), 2.46 (s, 3H, C_6H_4−CH_3), 2.25−2.13 (m, 1H, C*H*$(CH_3)_2$), 0.80 (d, ^3J = 6.5 Hz, 3H, CH(CH_3)$_2$), 0.49 (d, ^3J = 6.5 Hz, 3H, CH(CH_3)$_2$). ^{13}C NMR (75.5 MHz, $CDCl_3$) δ 167.17, 161.36, 145.26, 136.54, 132.61, 132.48, 129.98, 129.41, 129.12, 128.28, 128.03, 127.70, 114.65, 67.62, 65.76, 63.62, 48.63, 27.10, 21.72, 19.77, 19.16. MS (ESI-EM) *m*/*e*: 599.1487 $(M + Na)^+$ calcd for $C_{27}H_{32}N_2O_8S_2Na$ 599.1492. Anal. ($C_{27}H_{32}N_2O_8S_2$) C, H, N.

Radiochemistry. *Production of [^{18}F]Fluoride and Synthesis of [^{18}F]K(K 222)F.* No-carrier-added aqueous [^{18}F]fluoride was produced on a RDS 111e cyclotron (CTI-Siemens) by irradiation of a 1.2 mL water target using 10 MeV proton beams on 97.0% enriched [^{18}O]water by the ^{18}O(p,n)^{18}F nuclear reaction. Typical [^{18}F]fluoride ion batches were 9.4 GBq and 4.5 GBq for the two-step and one-step procedures at end of radionuclide production for currents of 32 μA and irradiation times of 12 and 4 min, respectively. To recover the [^{18}O]water, the batch of aqueous [^{18}F]fluoride was passed through an anion exchange resin (Sep-Pak Light Waters Accell Plus QMA cartridge, preconditioned with 5 mL of 1 M K_2CO_3 and 10 mL of water). [^{18}F]Fluoride was eluted from the resin with a mixture of 40 μL of 1 M K_2CO_3, 200 μL of water for injection, and 800 μL of DNA-grade CH_3CN containing 18 mg of Kryptofix 2.2.2 (K 222). Subsequently, the aqueous [^{18}F]K(K 222)F solution was carefully evaporated to dryness *in vacuo*.

(*R*)-2-(*N*-Benzyl-4-(2-[^{18}F]fluoroethoxy)phenylsulfonamido)-*N*-hydroxy-3-methylbutanamide ([^{18}F]1f) (Two-Step Procedure). An amount of 5.7 mg (9.0 μmol) of compound **6k** and the carefully dried [^{18}F]K(K 222)F residue were heated at 84 °C in 1 mL of DNA-grade acetonitrile for 4 min. The mixture was cooled to 40 °C, diluted with 10 mL of water for injection, and passed through a Waters Sep-Pak C18 cartridge. The cartridge was washed with 10 mL of water for injection and eluted with 4 mL of acetonitrile. Subsequently, the eluate was evaporated to dryness. Compound **[^{18}F]6h** was obtained in radiochemical yields of 39.5 ± 5.1% (decay-corrected, n = 5). An amount of 1 mL of trifluoroacetic acid (TFA) taken from a freshly opened ampule was then added. The reaction mixture was vortexed and refluxed for 20 min. TFA was evaporated, 350 μL of acetonitrile followed by 650 μL of water was added, and the resulting solution was purified using a gradient radio-HPLC procedure (conditions: λ = 254 nm; flow = 4 mL/min; eluents = A: CH_3CN/H_2O/TFA, 950/50/1 and B: CH_3CN/H_2O/TFA, 50/950/1; time program = eluent B from 70% to 30% in 30 min, halt 5 min, from 30% to 70% in 5 min). The product fraction of compound **[^{18}F]1f** (retention time t_R = 15.3 min) was evaporated to dryness *in vacuo* and redissolved with 1 mL of H_2O/EtOH (9:1). The second step provided the target compound **[^{18}F]1f** in radiochemical yields of 31.4 ± 6.5% (decay-corrected, n = 5). Product compound **[^{18}F]1f** was obtained in an overall radiochemical yield (two steps including synthesis of [^{18}F]K(K 222)F) of 12.4 ± 3.0% (decay-corrected) and a radiochemical purity of 97.3 ± 1.6% after 113 ± 6 min from end of radionuclide production. The determined specific radioactivity was 44 ± 19 GBq/μmol (32−72 GBq/μmol) at the EOS (n = 5). The specific activity of product **[^{18}F]1f** was estimated by comparing the peak area of purified **[^{18}F]1f** in the UV channel (retention time t_R = 11.8 min) with a standard curve of known concentrations of reference compound **1f** measured with a RP-HPLC system (conditions: λ = 254 nm; flow = 0.3 mL/min; eluent = CH_3CN/H_2O/TFA, 450/550/1). The chemical identity of **[^{18}F]1f** was proved by coinjection and coelution of **[^{18}F]1f** and the nonradioactive counterpart **1f** on the same HPLC system.

(*R*)-2-(*N*-Benzyl-4-(2-[^{18}F]fluoroethoxy)phenylsulfonamido)-*N*-hydroxy-3-methylbutanamide ([^{18}F]1f) (One-Step Procedure). An amount of 5.8 mg (10.0 μmol) of compound **1i** and the carefully dried [^{18}F]K(K 222)F residue were heated at 84 °C in 1 mL of DNA-grade CH_3CN for 20 min. The mixture was cooled to 40 °C, diluted with 10 mL of water for injection, and passed through a Waters Sep-Pak Light C18 cartridge. The cartridge was washed with 10 mL of water for injection and eluted with 0.4 mL of warm dimethylformamide (DMF) (warmed to 120 °C before elution). The eluate was diluted with 0.5 mL of water for injection and purified by HPLC (conditions: see two-step procedure). The product fraction

of compound **[^{18}F]1f** was evaporated to dryness *in vacuo* and redissolved with 1 mL of H_2O/EtOH (9:1). The radiosynthesis provided **[^{18}F]1f** with radiochemical yields of 45.6 ± 5.6% (decay-corrected, $n = 5$), a radiochemical purity of 95.5 ± 3.1% in 115 ± 10 min from end of radionuclide production, and a calculated specific radioactivity of 60 ± 25 GBq/μmol (42−97 GBq/μmol) at the EOS ($n = 5$).

Measurement of log *D* Values. The determination of the log *D* values of **[^{18}F]1f** and **[^{18}F]1j** was performed in 1-octanol and 0.02 M phosphate buffer at pH 7.4 as described previously.[35,36] The layers were counted in an automated gamma counter (Wallac Wizard 3″, Perkin-Elmer Life Sciences, Boston, MA), back correcting for decay. The measurement was repeated four times. The log *D* value was determined by calculating the ratio of 1-octanol to that of buffer.

$$\log D = \log\left(\frac{\text{cpm/mL octanol}}{\text{cpm/mL buffer}}\right)$$

***In Vitro* Enzyme Inhibition Assays.** The synthetic broad-spectrum fluorogenic substrate (7-methoxycoumarin-4-yl) acetyl pro-Leu-Gly-Leu-(3-(2,4-dinitrophenyl)-L-2,3-diamino-propionyl)-Ala-Arg-NH_2 (R & D Systems, Minneapolis, MN) was used to assay activated MMP-2, MMP-8, MMP-9, and MMP-13 as described previously.[37] The inhibitions of human active MMP-2, MMP-8, MMP-9, and MMP-13 by CGS 27023A, its nonradioactive analogues **1a**−**1f**, **1h**, and **1j**−**1n**, and the carboxylic acids **5a**−**5c**, **5f**, **5h**, and **5i**−**5l** were assayed by preincubating MMP-2 (2 nM), MMP-8 (2 nM), MMP-9 (2 nM), or MMP-13 (2 nM) and inhibitor compounds at varying concentrations (10 pM−1 mM) in 50 mM Tris·HCl, pH 7.5, containing 0.2 M NaCl, 5 mM $CaCl_2$, 20 μM $ZnSO_4$, and 0.05% Brij 35 at 37 °C for 30 min. An aliquot of substrate (10 μL of a 50 μM solution) was then added to 90 μL of the preincubated MMP/inhibitor mixture, and the fluorescence was determined at 37 °C by following product release with time. The fluorescence changes were monitored using a Fusion Universal Microplate analyzer (Packard Bioscience, MA) with excitation and emission wavelengths set to 330 and 390 nm, respectively. Reaction rates were measured from the initial 10 min of the reaction profile where product release was linear with time and plotted as a function of inhibitor dose. From the resulting inhibition curves, the IC_{50}-values for each inhibitor were calculated by nonlinear regression analysis, performed using the Grace 5.1.8 software (Linux).

Biodistribution. Animals were handled and maintained according to approved protocols of the animal welfare committees of the University of Münster, Germany.

Adult C57/BL6 mice (male and female, 21−30 g) were anesthetized by isoflurane/N_2O/O_2, and one lateral tail vein was canulated using a 27 G VenofixA needle with 15 cm polyethylene catheter tubing (od 1 mm, id 0.38 mm). Animals were allowed to recover from the anesthesia for ∼1 h, and during the studies they were conscious but under light restraint. Compounds **[^{18}F]1f** or **[^{18}F]1j** (13−32 MBq·kg^{-1}, 1−4 nmol·kg^{-1}) each were injected as a bolus (50−100 μL) via the tail vein. In some animals, unlabeled ligand (**1f** or **1j**) at >25 μmol·kg^{-1} was injected 10 min before the radioligand. Aliquots of each injectant were diluted in saline and measured to determine the radioactivity injected into each animal. At selected times after injection of the radioligand, the animals were sacrificed by intravenous injection of sodium pentobarbitone (Euthatal) at 200 mg·(kg body weight)$^{-1}$. Blood samples were taken by cardiac puncture, samples of urine and bile were taken by puncture of the urinary and gall bladders, respectively, and selected tissues were rapidly removed. Tissue samples were blotted dry with filter paper and transferred to weighed vials for reweighing and measurement of radioactivity using an automated gamma counter. Radioactivity was expressed as an uptake index, defined as

$$\text{uptake index} = \frac{\text{tissue radioactivity (cpm)/tissue wet weight (g)}}{\text{radioactivity injected (cpm)/body weight (g)}}$$

Metabolism. Adult C57BL/6 mice (male and female, 25−30 g) were prepared in accordance to the section on biodistribution (see above). Compounds **[^{18}F]1f** or **[^{18}F]1j** each were injected as a bolus (100 μL) via the tail vein. Aliquots of each injectant were diluted in saline and measured to determine the radioactivity injected into each animal. The animals were sacrificed at 2.5 or 20 min after injection of the radiotracer by intravenous injection of sodium pentobarbitone (Euthatal) at 200 mg·(kg body weight)$^{-1}$. Blood was taken immediately by cardiac puncture and centrifuged at 10 000*g* for 4 min to separate the plasma. Plasma from 2−3 (2.5 min) or 4 (20 min) mice was pooled for analysis by HPLC. Ice-cold acetonitrile (0.7 mL) was added to the pooled plasma (0.7−1.0 mL), and the precipitated proteins were removed by centrifugation (10 000*g* for 4 min). A sample of the resulting supernatant (900 μL) was spiked with nonradioactive **1f** or **1j** (10 μg) and analyzed by HPLC (conditions for **[^{18}F]1f**: $\lambda = 254$ nm; flow = 4 mL/min; eluents = A: CH_3CN/H_2O/TFA, 950/50/1 and B: CH_3CN/H_2O/TFA, 50/950/1; time program = eluent B from 70% to 30% in 30 min, halt 5 min, from 30% to 70% in 5 min, retention time t_R(polar metabolite) = 2.2 min, t_R(metabolite) = 11.5 min, t_R(**[^{18}F]1f**) = 13.3 min; conditions for **[^{18}F]1j**: $\lambda = 254$ nm; flow = 8 mL/min; eluents = A: CH_3CN/H_2O/TFA, 950/50/1 and B: CH_3CN/H_2O/TFA, 50/950/1; time program = eluent B from 92% to 30% in 45 min, halt 5 min, from 30% to 92% in 5 min, retention time t_R(polar metabolite) = 1.2 min, t_R(**[^{18}F]1j**) = 9.1 min).

At 20 min, the hearts and the right tibiae were removed and transferred to weighed vials for reweighing and measurement of radioactivity using an automated gamma counter. Radioactivity was expressed as uptake index (as defined above).

Acknowledgment. This work was supported by grants from the Deutsche Forschungsgemeinschaft (DFG), Sonderforschungsbereich 656, Münster, Germany (Project SFB 656 A2, A3 and B1). We gratefully acknowledge Sven Fatum for technical assistance and the BASF AG, Ludwigshafen, Germany, for kindly providing *O*-*tert*-butylhydroxylamine hydrochloride.

Supporting Information Available: Elemental analyses and ESI-EM data of target compounds and routine experimental and spectroscopic data of intermediates. This material is available free of charge via the Internet at http://pubs.acs.org.

References

(1) Skiles, J. W.; Gonnella, N. C.; Jeng, A. Y. The design, structure, and clinical update of small molecular weight matrix metalloproteinase inhibitors. *Curr. Med. Chem.* **2004**, *11*, 2911−2977.
(2) Tayebjee, M. H.; Lip, G. Y. H.; MacFadyen, R. J. Matrix metalloproteinases in coronary artery disease: Clinical and therapeutic implications and pathological significance. *Curr. Med. Chem.* **2005**, *12*, 917−925.
(3) Beaudeux, J. L.; Giral, P.; Bruckert, E.; Foglietti, M. J.; Chapman, M. J. Matrix metalloproteinases, inflammation and atherosclerosis: Therapeutic perspectives. *Clin. Chem. Lab. Med.* **2004**, *42*, 121−131.
(4) Whittaker, M.; Ayscough, A. Matrix metalloproteinases and their inhibitors-current status and future challenges. *Celltransmissions* **2001**, *17*, 3−14.
(5) Borkakoti, N. Structural studies of matrix metalloproteinases. *J. Mol. Med.* **2000**, *78*, 261−268.
(6) Stamenkovic, I. Extracellular matrix remodelling: The role of matrix metalloproteinases. *J. Pathol.* **2003**, *200*, 448−464.
(7) Rhee, J. S.; Coussens, L. M. RECKing MMP function: Implications for cancer development. *Trends Cell Biol.* **2002**, *12*, 209−211.
(8) Galis, Z. S.; Khatri, J. J. Matrix metalloproteinases in vascular remodeling and atherogenesis: The good, the bad, and the ugly. *Circ. Res.* **2002**, *90*, 251−62.
(9) George, S. J. Therapeutic potential of matrix metalloproteinase inhibitors in atherosclerosis. *Expert Opin. Invest. Drugs* **2000**, *9*, 993−1007.
(10) Brinckerhoff, C. E.; Matrisian, L. M. Matrix metalloproteinases: A tail of a frog that became a prince. *Nat. Rev. Mol. Cell Biol.* **2002**, *3*, 207−214.
(11) Rasmussen, H. S.; McCann, P. P. Matrix metalloproteinase inhibition as a novel anticancer strategy: A review with special focus on batimastat and marimastat. *Pharmacol. Ther.* **1997**, *75*, 69−75.

(12) Steward, W. P. Marimastat (BB2516): Current status of development. *Cancer Chemother. Pharmacol.* **1999**, *43*, S56−S60.
(13) Price, A.; Shi, Q.; Morris, D.; Wilcox, M. E.; Brasher, P. M.; Rewcastle, N. B.; Shalinsky, D.; Zou, H.; Appelt, K.; Johnston, R. N.; Yong, V. W.; Edwards, D.; Forsyth, P. Marked inhibition of tumor growth in a malignant glioma tumor model by a novel synthetic matrix metalloproteinase inhibitor AG3340. *Clin. Cancer Res.* **1999**, *5*, 845−854.
(14) Giersing, B. K.; Rae, M. T.; CarballidoBrea, M.; Williamson, R. A.; Blower, P. J. Synthesis and characterization of ^{111}In-DTPA-N-TIMP-2: A radiopharmaceutical for imaging matrix metalloproteinase expression. *Bioconjugate Chem.* **2001**, *12*, 964−971.
(15) Oltenfreiter, R.; Burvenich, I.; Staelens, L.; Lejeune, A.; Frankenne, F.; Foidart, J. M.; Slegers, G. Synthesis, quality control and *in vivo* evaluation of [^{123}I]rhTIMP-2, a potential tumour-imaging agent. *J. Labelled Compd. Radiopharm.* **2005**, *48*, 387−396.
(16) Li, W. P.; Lewis, J. S.; Lan, S.; Anderson, C. J. Cu-64-DOTA CTTHWGFTLC, a selective gelatinase inhibitor for tumor imaging. *J. Nucl. Med.* **2002**, *43*, S277−S278.
(17) Kulasegaram, R.; Giersing, B.; Page, C. J.; Blower, P. J.; Williamson, R. A.; Peters, B. S.; O'Doherty, M. J. *In vivo* evaluation of ^{111}In-DTPA-N-TIMP-2 in Kaposi sarcoma associated with HIV infection. *Eur. J. Nucl. Med.* **2001**, *28*, 756−761.
(18) Li, W. P.; Lewis, J. S.; Eiblmaier, M.; Lan, S.; Anderson, C. J. *In vitro* and *in vivo* evaluation of a radiolabelled gelatinase inhibitor for microPET imaging of metastatic breast cancer. *Mol. Imaging Biol.* **2002**, *4*, S23.
(19) Spargue, J. E.; Li, W. P.; Liang, K.; Achilefu, S.; Anderson, C. J. *In vitro* and *in vivo* investigation of matrix metalloproteinase expression in metastatic tumor models. *Nucl. Med. Biol.* **2006**, *33*, 227−237.
(20) Wagner, S.; Breyholz, H.-J.; Faust, A.; Höltke, C.; Levkau, B.; Schober, O.; Schäfers, M.; Kopka, K. Molecular imaging of matrix metalloproteinases *in vivo* using small molecule inhibitors for SPECT and PET. *Curr. Med. Chem.* **2006**, *13*, 2819−2838.
(21) MacPherson, L. J.; Bayburt, E. K.; Capparelli, M. P.; Carroll, B. J.; Goldstein, R.; Justice, M. R.; Zhu, L.; Hu, S. I.; Melton, R. A.; Fryer, L.; Goldberg, R. L.; Doughty, J. R.; Spirito, S.; Blancuzzi, V.; Wilson, D.; O' Byrne, E. M.; Ganu, V.; Parker, D. T. Discovery of CGS 27023A, a non-peptidic, potent, and orally active stromelysin inhibitor that blocks cartilage degradation in rabbits. *J. Med. Chem.* **1997**, *40*, 2525−2532.
(22) Scozzafava, A.; Supuran, C. T. Carbonic anhydrase and matrix metalloproteinase inhibitors: sulfonylated amino acid hydroxamates with MMP inhibitory properties act as efficient inhibitors of CA isozymes I, II, and IV, and *N*-hydroxysulfonamides inhibit both these zinc enzymes. *J. Med. Chem.* **2000**, *43*, 3677−3687.
(23) Kopka, K.; Breyholz, H.-J.; Wagner, S.; Law, M. P.; Riemann, B.; Schröer, S.; Trub, M.; Guilbert, B.; Levkau, B.; Schober, O.; Schäfers, M. Synthesis and preliminary biological evaluation of new radioiodinated MMP inhibitors for imaging MMP activity *in vivo*. *Nucl. Med. Biol.* **2004**, *31*, 257−267.
(24) Schäfers, M.; Riemann, B.; Kopka, K.; Breyholz, H.-J.; Wagner, S.; Schäfers, K. P.; Law, M. P.; Schober, O.; Levkau, B. Scintigraphic imaging of matrix metalloproteinase activity in the arterial wall *in vivo*. *Circulation* **2004**, *109*, 2554−2559.
(25) Zheng, Q. H.; Hutchins, G. D.; Mock, B. H.; Winkle, W. L. MMP inhibitor radiotracer [^{11}C]Methyl-CGS 27023A: A new PET breast cancer imaging agent. *J. Labelled Compd. Radiopharm.* **2001**, *44*, S104−S106.
(26) Fei, X.; Zheng, Q. H.; Hutchins, G. D.; Liu, X.; Stone, K. L.; Carlson, K. A.; Mock, B. H.; Winkle, W. L.; Glick-Wilson, B. E.; Miller, K. D.; Fife, R. S.; Sledge, G. W.; Sun, H. B.; Carr, R. E. Synthesis of MMP inhibitor radiotracers [^{11}C]methyl-CGS 27023A and its analogs, new potential PET breast cancer imaging agents. *J. Labelled Compd. Radiopharm.* **2002**, *45*, 449−470.
(27) Zheng, Q. H.; Fei, X.; Liu, X.; Wang, Q. J.; Sun, H. B.; Mock, B. H.; Stone, K. L.; Martinez, T. D.; Miller, K. D.; Sledge, G. W.; Hutchins, G. D. Synthesis and preliminary biological evaluation of MMP inhibitor radiotracers [^{11}C]methyl-halo-CGS 27023A analogs, new potential PET breast cancer imaging agents. *Nucl. Med. Biol.* **2002**, *29*, 761−770.
(28) Fei, X.; Zheng, Q. H.; Liu, X.; Wang, J. Q.; Stone, K. L.; Miller, K. D.; Sledge, G. W.; Hutchins, G. D. Synthesis of MMP inhibitor radiotracer [^{11}C]CGS 25966, a new potential PET tumor imaging agent. *J. Labelled Compd. Radiopharm.* **2003**, *46*, 343−351.
(29) Zheng, Q. H.; Fei, X.; Liu, X.; Wang, J. Q.; Stone, K. L.; Martinez, T. D.; Gay, D. J.; Baity, W. L.; Miller, K. D.; Sledge, G. W.; Hutchins, G. D. Comparative studies of potential cancer biomarkers carbon-11 labeled MMP inhibitors (*S*)-2-(4′-[^{11}C]methoxybiphenyl-4-sulfonylamino)-3-methylbutyric acid and *N*-hydroxy-(*R*)-2-[[(4′-[^{11}C]methoxyphenyl)sulfonyl]benzylamino]-3-methylbutanamide. *Nucl. Med. Biol.* **2004**, *31*, 77−85.
(30) Breyholz, H.-J.; Wagner, S.; Levkau, B.; Schober, O.; Schäfers, M.; Kopka, K. A ^{18}F-radiolabelled analogue of CGS 27023A as a potential agent for assessment of matrix-metalloproteinase activity *in vivo*. *Q. J. Nucl. Med. Mol. Imaging* **2007**, *51*, 24−31.
(31) Lasne, M.-C.; Perrio, C.; Rouden, J.; Barré, L.; Roeda, D.; Dollé, F.; Crouzel, C. Chemistry of β^+-emitting compounds based on fluorine-18. *Top. Curr. Chem.* **2002**, *222*, 201−258.
(32) Smith, C.; Porter, B.; Walsh, R.; Majid, T.; McCarthy, C.; Harris, D; Astles, P.; McLay, I.; Morley, A.; Bridge, A.; Van Sickle, A.; Halley, F.; Roach, A.: Foster, M. (Rhone-Poulenc Rorer Ltd.). Substituted phenyl compounds with a substituent having a 1,3-benzodioxole ring. U.S. Patent 6034893, April 11, 2000.
(33) Mutschler, E. *Arzneimittelwirkungen*; wissenschaftliche Verlagsgesellschaft mbH: Stuttgart, 1996; pp 20−34.
(34) Caldarelli, M.; Habermann, J.; Ley, S. V. Synthesis of an array of potential matrix metalloproteinase inhibitors using a sequence of polymer-supported reagents. *Bioorg. Med. Chem. Lett.* **1999**, *9*, 2049−2052.
(35) Wilson, A. A.; Jin, L.; Garcia, A.; DaSilva, J. N.; Houle, S. An admonition when measureing the lipophilicity of radiotracers using counting techniques. *Appl. Radiat. Isot.* **2001**, *54*, 203−208.
(36) Wilson, A. A.; Houle, S. Radiosynthesis of carbon-11 labelled *N*-Methyl-2-(arylthio)benzylamines: Potential radiotracers for serotonin reuptake receptors. *J. Labelled Compd. Radiopharm.* **1999**, *42*, 1277−1288.
(37) Huang, W.; Meng, Q.; Suzuki, K.; Nagase, H.; Brew, K. Mutational study of the amino-terminal domain of human tissue inhibitor of metalloproteinasees 1 (TIMP-1) locates an inhibitory region for matrix metalloproteinases. *J. Biol. Chem.* **1997**, *272*, 22086−22091.

JM0708533